Review—Practical Challenges Hindering the Development of Solid State Li Ion Batteries

Review—Practical Challenges Hindering the Development of Solid State Li Ion Batteries

Kian Kerman,[a,z] Alan Luntz,[a,*] Venkatasubramanian Viswanathan,[b] Yet-Ming Chiang,[c,*] and Zhebo Chen[a,*]

[a]*SUNCAT Center for Interface Science and Catalysis, Department of Chemical Engineering, Stanford University, Stanford, California 94305, USA*
[b]*Department of Mechanical Engineering, Carnegie Mellon University, Pittsburgh, Pennsylvania 15213, USA*
[c]*Department of Materials Science and Engineering, Massachusetts Institute of Technology, Cambridge, Massachusetts 02139, USA*

Solid state electrolyte systems boasting Li^+ conductivity of >10 mS cm^{-1} at room temperature have opened the potential for developing a solid state battery with power and energy densities that are competitive with conventional liquid electrolyte systems. The primary focus of this review is twofold. First, differences in Li penetration resistance in solid state systems are discussed, and kinetic limitations of the solid state interface are highlighted. Second, technological challenges associated with processing such systems in relevant form factors are elucidated, and architectures needed for cell level devices in the context of product development are reviewed. Specific research vectors that provide high value to advancing solid state batteries are outlined and discussed.
 [DOI: 10.1149/2.1571707jes]

Manuscript submitted March 20, 2017; revised manuscript received May 26, 2017. Published June 9, 2017.

Solid state battery systems are of great interest because of potential benefits in gravimetric and volumetric energy density, operable temperature range, and safety in comparison to traditional liquid electrolyte based systems. However, unresolved fundamental issues remain in the quest to fully understand the behavior of all-solid batteries, especially in the area of electrochemical interfaces.[1] There are also a number of significant engineering challenges that require methodical effort to enable a tangible product. Some transitions from academic laboratories to entrepreneurial efforts attempting to overcome these challenges remain unsuccessful in efforts to bring a product to the market.[2,3] Vital parameters that require robust understanding from a product development standpoint are material cost, cell lifetime and shelf life, cell energy density on a volumetric and gravimetric basis, operable capabilities for given temperature conditions, and safety. The advantage of energy density remains to be realized in solid state electrolytes (SSEs) since most studies to date utilize thick SSEs or cathodes with low active loading compared to liquid counterparts.[4,5] Furthermore, the desire to use SSEs in conjunction with Li metal anodes requires understanding and managing the morphology of Li metal plating, which can impact volumetric energy density. Operation at both higher and lower temperature compared to conventional technologies is a significant potential advantage of SSE systems. However, reports of solid state cells achieving parity with traditional systems at room temperature or any other temperature do not currently exist. The safety, specifically decreased flammability, of SSE systems is another potential advantage but requires ongoing validation and study.[6] Unlike current liquid electrolyte systems,[7] the manufacturability and material component costs of SSEs have not been well characterized, and thus the value of these features will need to be weighed accordingly with any added cost. Operating lifetime of SSEs capturing intrinsic materials parameters such as voltage stability,[8] as well as catastrophic failure modes such as shorting,[9] have been briefly investigated, but in the absence of high energy density electrode formulations and application based testing protocols that are comparable to commercial liquid electrolyte cells. To enable development and maturation of solid state battery technology, the value propositions of SSEs must be substantiated with relevant data in the coming years. Companies with competencies in ceramic or battery processing and with the resources to engage in a broad level of materials development and failure analysis may be well positioned to enable this technology. This work outlines, reviews, and highlights critical pragmatic research areas that could provide high value in developing solid state battery systems.

*Electrochemical Society Member.
[z]E-mail: kiankerman@post.harvard.edu

Several reviews have tackled the topic of solid state battery technology from various perspectives.[10–19] Sun et al. provide a detailed overview of updates in the field,[10] while Manthiram et al. give an academic overview of technologies that could benefit from solid state electrolytes.[11] The following discussion takes the unique perspective of identifying critical research areas that need significant development, particularly related to material processing in relevant form factors. For the purposes of this review, two well studied systems, namely $Li_7La_3Zr_2O_{12}$ (LLZO) and xLi_2S-yP_2S_5 (LPS) as well as their derivatives, are used to frame the discussion on mechanics, processing, and full cell integration challenges. A discussion of other candidate classes such as anti-perovskites, halides, and nitrides is also given. The overall material development challenges discussed are applicable across these solid electrolyte classes. A comprehensive review of doping strategies, structural effects, conductivity, and status of LLZO type lithium ion conductors can be found elsewhere.[20] Information on LPS and other sulfide based electrolyte systems can also be found in focused subject reviews.[21] An overview of fundamentals in ionic conduction properties in many SSEs has been recently outlined.[18] Although a large bulk of the literature in the field of SSEs is focused on improving conductivity of varying material compositions, it is noted that high conductivity is a necessary but insufficient property. While processing parameters can have significant effects on properties such as conductivity, this discussion is not focused on optimization of a single parameter, but instead takes a holistic approach to developments necessary for a robust product.

Solid Electrolyte Mechanical Considerations

Solid electrolytes are of keen interest in part due to proposed dendrite or Li penetration resistance that could enable the use of a Li metal electrode. This section introduces basic material properties of SSEs and importantly highlights key differences in theory and understanding of material physics required for failure-resistant SSE materials compared to other electrolytes.

Dense LLZO type materials prepared by hot pressing techniques have been mechanically evaluated by ultrasound spectroscopy and indentation methods,[22,23] and are found to exhibit an elastic modulus of 150 GPa and fracture toughness of 0.86 – 1.63 MPa $m^{0.5}$. High density LPS type materials prepared by hot pressing techniques evaluated as a function of xLi_2S-yP_2S_5 compositional ratio show elastic moduli of 18–25 GPa.[24] While there are examples of macroscopic deformability in LPS type materials, they are brittle in nature as exemplified by a low fracture toughness of 0.23 MPa $m^{0.5}$.[25] Though unstable to Li, $Li_{1.2}Zr_{1.9}Sr_{0.1}(PO_4)_3$ has been reported to show an elastic modulus

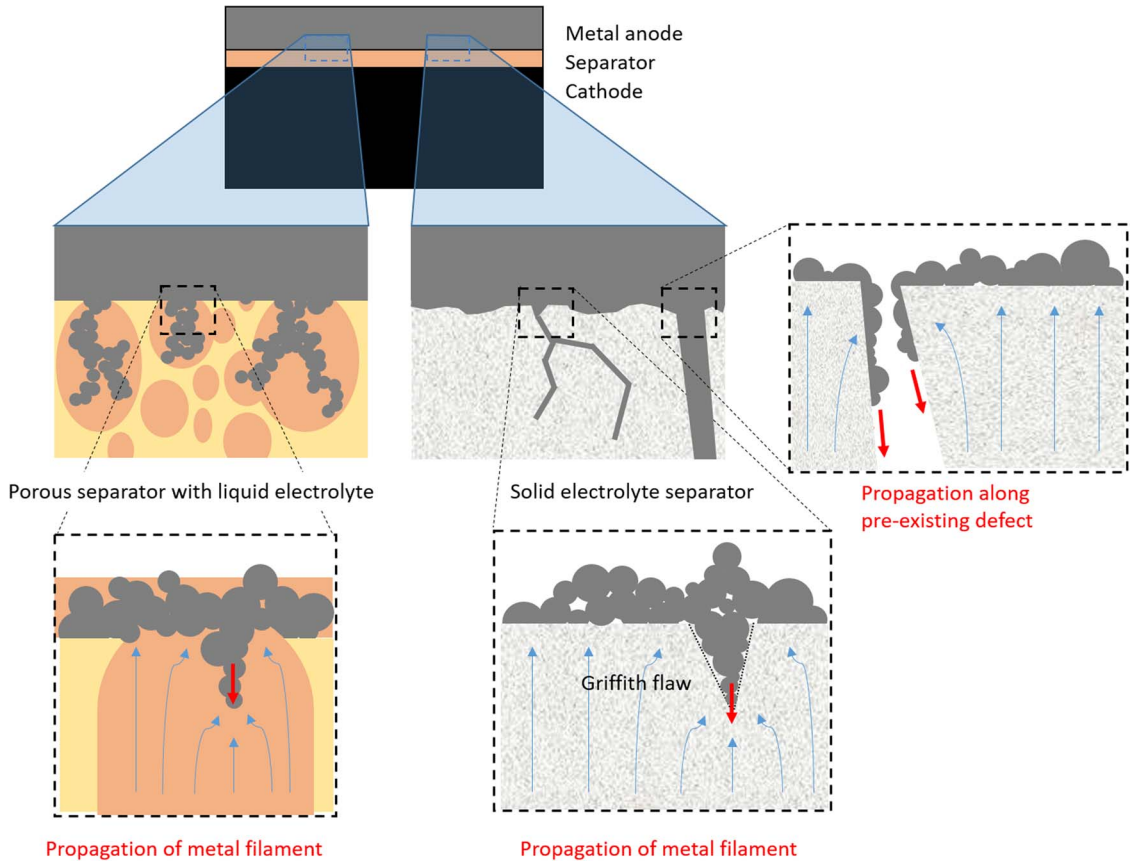

Figure 1. Illustration of Li metal electrodeposition in liquid electrolytes and solid state electrolytes. Red arrows point toward undesired metal growth into the bulk of the separator and blue arrows show electric field lines. For simplicity, the current collector is omitted and metal is depicted with circular morphology. A defect mediated failure mechanism of Li penetration in SSEs is emphasized as opposed to classic 'dendritic' growth.

of 40 GPa and fracture toughness of 0.37 MPa $m^{0.5}$.[26] For reference, the elastic and shear modulus of bulk Li metal is 4.9 and 4.2 GPa, respectively.

There are several methods that have been suggested for suppression of Li penetration at the Li-solid electrolyte interface. Monroe and Newman considered a solid polymer electrolyte in contact with a Li metal electrode. Using linear stability analysis it was shown that materials with roughly twice the shear modulus of lithium could suppress dendrites at the Li-solid polymer interface.[27] This approach has led to enormous interest in the development of high shear modulus solid electrolytes.[10,13,14,16,19] Another route suggested is to increase stresses at the interface beyond the yield strength of lithium so the anode can plastically deform and planarize.[28] It may also be possible to trigger this deformation by applying an external pressure perpendicular to the cell stack greater than the yield strength of Li. An alternative analysis shows that electrodeposition leads to a change in the density of lithium, which can impact hydrostatic stress and affect the critical shear modulus needed to establish Li stability.[29] Two distinct stability mechanisms to prevent Li penetration may exist: pressure-driven, relevant for solid-polymer electrolytes with larger partial molar volume of lithium, and density-driven, relevant for SSEs with lower partial molar volume of lithium. For a pressure-driven stability mechanism, critical shear modulus needs to be higher than that of lithium, as supported by the Monroe-Newman model. For a density driven stability mechanism relevant to SSEs, critical shear modulus may need to be lower than that of lithium, although this requires experimental validation.

Pragmatically, the criterion discussed above is conceptually aimed at the initiation of dendrites from an initial condition where the interface is smooth and flat. This may apply to electrolytes formed in a manner producing interfaces that are atomically smooth, for example vapor-deposited LiPON. However, for typical SSEs, an alternative failure mode is the propagation of pre-existing interfacial defects, namely Griffith flaws.[30] During electrodeposition through the solid electrolyte, such interfacial flaws are the first to fill with metal, schematically shown in Figure 1. As additional metal arrives at the tip of the flaw where electric field is largest, a competition arises between propagation of the metal filament into the solid electrolyte and extrusion of the metal backwards, to accommodate volume increase. It can be shown that for any reasonable aspect ratio (length to width) of the flaw, the stress to open the crack is reached well before that required for backwards flow of the metal,[31] valid even at the very low yield stress of bulk Li metal. Schmidt and Sakamoto report in-situ acoustic experiments related to this mechanism finding that a reduction in SSE stiffness accompanies Li penetration, consistent with crack propagation.[30] According to this theory, the ability of all-solid-state batteries to cycle without Li penetration related failures is predicated on defect-free layers. Correspondingly, the growing number of observations of metal penetration through high modulus SSEs, observed in cycling of Li symmetric cells,[9,33–35] can likely be explained by pre-existing interfacial defects. Another consideration is that Li metal at the nanoscale may exhibit yield stresses that are greater than bulk Li,[32] requiring even higher modulus SSEs.

Materials Fabrication

Given that minimizing critical defect densities in SSEs is of the utmost importance, processing is intimately linked to component reliability and practical feasibility. Defects can be loosely defined as any non-uniformity at the macroscopic level, including large-scale porosity or cracks, or at the microscopic level, such as pore channels at multi-grain junctions, grain boundaries, impurity precipitates, or even

Figure 2. Images of highly dense LLZO material exhibiting varying degrees of translucency depending on the density of defects within the sintered material. (a) Thin film made by tape casting reproduced from Reference 38 with permission from the Royal Society of Chemistry; (b) a bulk ceramic piece processed by pressure assisted sintering reproduced from Reference 39 with permission from the American Chemical Society; and (c) a bulk ceramic LLZO piece exhibiting partial areas of high density made with hot isostatic sintering methods reproduced from Reference 33 with permission from Elsevier.

local non-stoichiometry. SSE materials, shown in Figure 2, displaying translucency can be considered simple examples of low macroscopic defect density,[33,36–39] exhibiting low levels of optical scattering defects. However, it is not clear that even such materials are sufficiently defect-free as to avoid Li metal penetration. SSEs such as LLZO, LPS, anti-perovskites, and hydrides can be made using various synthetic approaches broadly outlined in Figure 3. One general approach involves taking solid precursor powders, homogenizing and processing the mixture using various formulation schemes, followed by deposition methodologies used in conventional battery manufacturing. A well-established technique for forming thin ceramic bodies, such as tape casting, is an excellent candidate for developing adequately thin SSEs.[40] Complexities that can arise in such a process include the selection of compatible binder and solvent systems, the incoming particle size distribution, and maintaining planarity upon final densification. Thin, free standing films will also require attention regarding surface compositional changes, physical shrinkage, warpage, sticking, and breakage.[41]

Many of these materials can also be made using vapor deposition processes, such as pulsed laser deposition (PLD), physical vapor deposition (PVD), chemical vapor deposition (CVD), and atomic layer deposition (ALD), although aspects of cost and scalability using such methods require additional consideration. Anti-perovskites, for example Li_3OCl, and hydrides, such as $LiBH_4$, can melt at temperatures below 300°C.[42,43] This introduces an alternative method of producing electrolyte films, although the thermal stability of any co-processed cell components must be taken into consideration. In many of these systems, significant effort is required to ensure an inert environment during materials synthesis, cell assembly, and subsequent usage to prevent undesired oxidation. Maintaining an inert environment is non-trivial and can lead to significant manufacturing cost as well as difficulty in mass producing quality material with high yield.

In order to use a high energy density anode such as Li metal or Si, the final SSE must be thin enough to reach total resistance and physical volume comparable to those from a porous separator and liquid

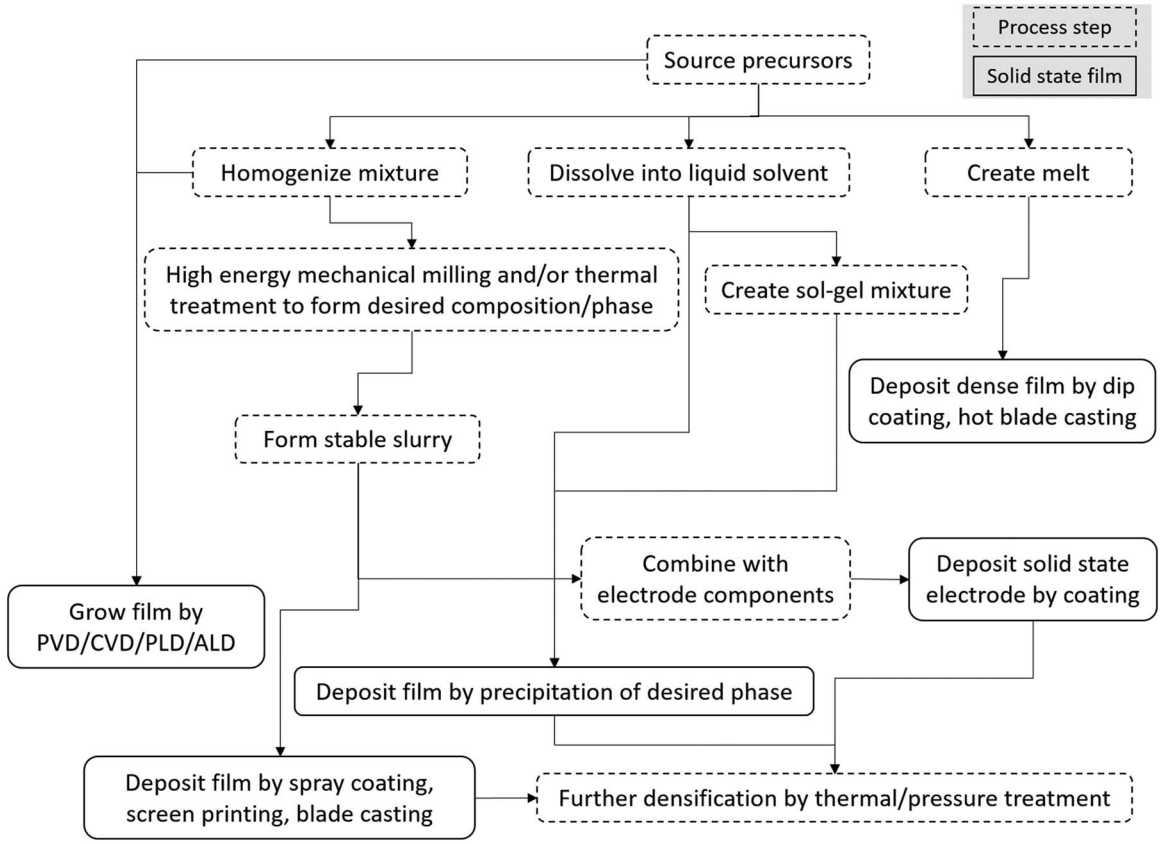

Figure 3. A broadly applicable process flow diagram for creating dense solid state electrolyte materials in the relevant form factors (<100 μm thickness) for competitive solid state battery devices. Each material family has specific processing details and examples outlined in the text.

electrolyte. The total SSE resistance is the sum of the resistances of the bulk material, the SSE-anode interface, and the SSE-cathode interface. For ionic conductivities of $\sim 5 \times 10^{-3}$ S cm^{-1}, SSE thicknesses in the <100 μm range are necessary to minimize bulk resistance and enable cell energy densities competitive with conventional Li ion technology.[44] Typical separators used with liquid electrolytes are ≤25 μm.[45] Since higher capacity cathodes and anodes require higher current densities to maintain the same C-rate, all else being equal, a lower bulk SSE resistance is required, which can only be achieved by SSE thickness reduction if electrolyte chemistry is fixed. This poses significant challenges for developing scalable manufacturing processes and may be one of the most serious hurdles facing solid state battery technology. The following discusses the background and challenges of processing dense, defect free solid Li ion conductors using LLZO and LPS as prototypical examples. Bulk processing and material forming can be used as a learning tool in understanding these systems and their fundamental limitations; however, a <100 μm thick form factor is ultimately required for technologically relevant devices.[44]

Processing of oxide-based SSEs.—*General process flow for bulk oxide preparation.*—Metal oxide compounds can be synthesized in a variety of ways.[46] All existing processes for SSEs, apart from vapor phase deposition of LiPON, typically begin with either a physical mixing method such as solid state reaction or chemical solution methods such as co-precipitation for the preparation of a starting powder. The complexities of these approaches are not discussed in detail here, but important considerations are cost, scalability,[47] and quality of powder produced. Due to the nature of oxide processing and the non-deformable property of refractory particles, considerable attention must be focused on particle size, morphology, and size distribution. Furthermore, unlike traditional ceramics such as Al_2O_3 or ZrO_2, LLZO or other Li conducting oxides require care in selecting processing solvents as they may cause unwanted diffusion of components during wet processing.[48,49] Similarly, reaction with the solvent may produce ionically insulating surface layers, such as carbonates, on particles in solution, complicating subsequent sintering.[50–52]

The successful sintering of metal oxides to high density requires control of multiple process parameters, and processes must typically be tuned to the specific compound being sintered.[53] Here, factors of importance based on LLZO are highlighted. Subtle variations in process parameters can have a large impact on the final sintered density, ionic conductivity, and failure resistance. When a conventional sintering approach using organic binder is conducted, it is important to have a homogenous distribution of the binder, as well as controlled and complete pyrolysis of the binder during the de-binding step, since residual contaminants can lead to porosity that cannot be closed during final stage sintering.[54] The substantial vapor pressure of Li at elevated temperature can lead to an outward flux of Li (as lithium oxide) that alters the final stoichiometry of the sintered body.[55] One solution is to formulate the starting compositions with an excess of Li in order to compensate for the evaporative loss and arrive at the desired phase and stoichiometry after sintering. Typical batching of 20–50% excess have been reported by teams developing highly dense samples.[33,38,56] Like many other ceramics, the gaseous environment; i.e. oxygen partial pressure, must also be optimized for a given stoichiometry.[53] Control of the starting particle size and morphology is important for developing a high final sintered density in ceramic systems, and methodologies to create tight particle size distributions of nanoparticles such as flame spray pyrolysis have been shown to be largely successful in this regard.[38]

Like previously well-studied high performance ceramic systems that contain a volatile cation, such as $Pb(Zr_xTi_{1-x})O_3$ (PZT),[57] the stoichiometry of sintered surfaces will likely be deficient in volatile species, namely Li, for LLZO type materials. Removal of this non-stoichiometric surface via plasma cleaning, ablation, or polishing of the sintered bodies may help improve chemical homogeneity and engineer surface roughness, both of which are critical for high quality interfacial contact. X-ray photoelectron spectroscopy studies show that a post-sintering process to create a pristine mating surface to the Li metal, such as polishing and processing of sintered bodies in a controlled Ar atmosphere, can be significant in reducing Li ion interfacial resistance due to surface carbonate formation.[51]

Meeting thickness requirements with oxide SSEs.—Figure 3 illustrates potential paths to forming LLZO having thickness <100 μm. PVD growth techniques such as sputtering[58] or PLD[59,60] have been demonstrated at research scale, but pose concerns from a scalability and cost perspective. For thin film micro-batteries, these approaches have been useful for deposition of SSEs films having thicknesses of 0.2–1 μm. Techniques such as ALD may also be useable for small cell designs. Recently, LiPON and LLZO were fabricated using ALD and custom precursor streams.[61,62] Conformity and tolerance to rough substrate surfaces are some key advantages that ALD can provide in contrast to PVD methods. Spin-coating of sol-gel precursors is another potential thin film deposition approach.[63,64] Laser assisted CVD of LLZO has also been demonstrated, though relatively low ionic conductivity of 4×10^{-6} S cm^{-1} was reported at 25°C.[65]

When using fine powders as the starting form of the SSE, tape casting is a plausible method for forming thin, dense oxide films at scale, analogous to processes used in the well-established multi-layer ceramic capacitor industry.[38,40,60,66] Like the bulk powder process described above, cast films require elevated temperature steps to remove binder and sinter to full density. As alluded to previously, free standing films require attention to surface compositional changes, physical shrinkage, warpage, sticking, and breakage at thin length scales.[41] In contrast to bulk materials that utilize a number of processes including mechanical polishing to address Li deficiencies at near-surface regions, thin bodies of brittle oxides are unlikely to withstand such post-fabrication processes. Thus, developing a method to maintain high Li vapor pressure while simultaneously maintaining film flatness during sintering is critical. Lessons from other oxide ceramic systems point to using sacrificial material to increase local vapor pressure of the volatile component near the surface of samples and planar stack structures for flatness.[57,67,68] Methods practiced by the solid oxide fuel cell community such as creating a porous metallic scaffold which supports a dense thin film to increase electrode surface area and provide structural support may also be explored using a co-sintering process.[69–71] The degree of porosity, ranging from fully dense to porous, needs to be optimized for performance and cell energy density[71–75]

Processing of sulfide-based SSEs.—*General process flow for bulk sulfide preparation.*—The sulfide compounds (often referred to as Thio-LISICON) can be processed in a manner similar to the oxides (see Figure 3), with some important exceptions. At the most upstream end of the process, precursor availability and safety are noteworthy considerations.[47] While not discussed in detail here, care must be taken to develop processes that utilize abundant and safe components in order to enable widespread adoption.

The atmosphere in which sulfide materials are processed require special consideration. These compounds are extremely sensitive to environment, and specifically, the ambient moisture content. Some sulfide components can react with atmospheric H_2O to form H_2S, a highly toxic compound. Li_2S and P_2S_5 are amongst the commonly used precursors for Thio-LISICON materials that can hydrolyze in the presence of moisture to form H_2S. Some studies have shown the benefit of using alternative precursors such as As_2S_5 and dopants such as ZnO to mitigate reactivity,[76,77] although the utilization of highly toxic metals such as arsenic is another concern. Atmospheric exposure also results in degradation of physical properties such as conductivity.[78] As such, controlled atmospheres are typically needed to prepare these materials and pose a substantial cost concern due to the need for strictly controlled formulation and packaging environments. From a product development perspective, adequate downstream engineering controls are necessary for full battery systems since the severity of a field failure is compounded if there is release of a gaseous toxin.

Once sulfide precursors are batched, formation of the desired high-conductivity phase can typically be obtained via thermal annealing, melt-quench, or high energy mechanical milling methods.[79] These processes operate broadly across the 25–1000°C temperature range and are potentially industrially scalable.[80] Certain compositions in the Li_2S–P_2S_5 space can be made at low temperatures in the range of 150–300°C,[81–83] while others, such as compositions in the Li_2S–SiS_2 space, are formed by quenching (for example, by the twin-roller method) from temperatures in excess of 900°C.[84–87] One of the unique and desirable attributes of the sulfide families of SSEs is their ability to be consolidated under pressure at low temperatures, even room temperature. Their deformation properties, wholly different from their oxide counterparts,[24,25] facilitate the consolidation of sulfide SSEs into dense bodies of various geometric form factors and the resulting increase in bulk density can increase conductivity.[88–90] Doped LPS of congruently melting compositions, such as the argyrodite (Li_6PS_5X where X = Cl, Br, I) family, can exhibit superior conductivity and electrochemical stability in comparison to pure LPS counterparts.[91–95] These compositions have mixed glassy and crystalline phase mixtures, which may present additional challenges to produce consistently at large scale. Improved understanding of the complex mix of structures and their phase stability regimes is imperative, but still in its early stages.[96,97]

Meeting thickness requirements with sulfide SSEs.—While the sulfide materials family boasts high ionic conductivity and simple bulk processing routes leading to highly dense bodies, processing the material in a relevant thin form factor remains a daunting task. PVD techniques that have been explored include sputtering[98] and PLD.[99] Thermal evaporation of elemental sources of the component materials, similar to processing of chalcogenide based solar materials such as $CuInGaSe_2$,[100] could also be performed.[101] In addition to obtaining dense films on non-uniform surfaces such as electrodes, engineering the crystal structure and ratio of crystalline to amorphous phase in these structurally complex materials requires significant effort. Solvent based techniques such as aerosol deposition or solution casting are attractive from a manufacturing standpoint, but compositional and phase control are likely more difficult due to the high propensity for polysulfide dissolution in the solvent.[102,103] Electrophoretic deposition is a non-traditional battery processing technique that could prove to be fruitful for forming a thin sulfide SSE.[104] At present, reports on synthesizing and implementing highly dense sulfide SSEs in relevant form factors using a scalable process remain sparse.

Processing of halide, hydride, and nitride systems.—A path not typically discussed in the context of oxide and sulfide materials is direct melt processing. Anti-perovskites, such as Li_3OCl and Li_3OBr families, can be melt processed at temperatures below 300°C.[42] Bulk Li_3OCl and doped isomorphs are readily prepared from solid-state reactions, such as $LiCl + 2LiOH \rightarrow Li_3OCl + H_2O$, at high temperatures and pressures in a closed reactor followed by drying with typical synthesis conditions of T > 230° C, but may require reaction times of several days,[42,105] Li_3OCl and its isomorphs possess a low melting temperature of $T_m = 282$°C, making melt-casting processes accessible. Recent work from Braga et al. highlights the low enthalpy of migration and 'wettability' of Li metal in $Li_{2.99}Ba_{0.005}O_{1+x}Cl_{1-2x}$.[106] It is strongly emphasized that processability and scalability must be considered. Aspects that require additional work include determining the role of H_2O and Li defects in such systems and reproducibly manufacturing anti-perovskite materials.[107] Films of Li_3OCl have been successfully fabricated via PLD from a composite target, achieving room temperature ionic conductivity of 2×10^{-4} S cm^{-1}.[108]

Hydrides, such as $LiBH_4$ and doped derivatives, can also be melt processed in similar fashion to anti-perovskites. Un-doped $LiBH_4$ has a $T_m = 277$°C, but decomposes above 300°C,[43] resulting in a tight processing window. Additionally, these materials are also known to be excellent H_2 storage candidates,[109,110] and hydrogen release can make elevated temperature processing precarious.

Nitrides, such as Li_3N and derivatives, have been well studied in single and poly crystalline form.[111–113] The most widely utilized synthesis route is a process that reacts molten Li with flowing N_2 gas at temperatures ranging from 180–800°C for reaction times of minutes to days.[114–116] While conductivity values of $\sim 6 \times 10^{-4}$ S cm^{-1} have been reported,[112] Li_3N has a prohibitively high electronic conductivity leading to intolerable self-discharge rates,[117] as well as limited voltage stability.[118,119] Without modification, it can be utilized against the anode in conjunction with a blocking layer interfacing with the cathode.[116]

Recent work has re-investigated the Li_3N system with the addition of SiS_2 using a mechano-chemical synthesis approach similar to that used for the sulfide families.[120] In this work, Iio et al. showed room temperature Li ion conductivity of $\sim 10^{-4}$ S cm^{-1}. Composites of $xLiBH_4$-Li_3N ($x = 1, 2, 4$) have also been synthesized in an effort to increase the stable voltage window of Li_3N.[121] It was shown that the material could be stable up to 3 V (vs. Li), though ionic conductivity was limited to 1×10^{-5} S cm^{-1}.

Ultimately, considering how SSEs will interface with other cell components is crucial for selecting a method to process materials in the proper form factor. Therefore, the full cell architecture should be used as a guide to the development of SSE geometry, processing techniques, and integration methods. A holistic view of the targeted battery system must be kept in mind when carrying out fundamental materials development.

Solid Electrolyte Interfaces

A fundamental requirement of any SSE-electrode interface is that it be chemically and electrochemically stable at the applicable potential. Since no SSE is simultaneously stable at both the reductive potentials of ~0 V (vs Li) at the negative electrode and at typical positive electrode potentials of ~4 V,[122] a stable, ionic conducting and self-limiting solid electrolyte interphase (SEI) must be formed, even by artificial means.[123–125] Beyond these considerations of electrochemical side reactions, the following discussion aims to provide focus on other key issues that affect interfacial stability.

Failure modes related to interfaces.—As in traditional liquid electrolyte systems, there are a number of failure modes that can occur due to phenomena at the solid electrolyte-electrode interface. The severity of SSE failure modes can range from catastrophic, such as an electrical short, to poor performance, such as low achieved capacity. Figure 4 summarizes some cell level consequences that can occur based on fundamental material physics, and potential solutions with associated product risks.

Interfacial delamination.—Volume expansion/contraction occurs throughout the state of charge for both the anode and the cathode. Conventional intercalation cathodes such as $LiCoO_2$ and $LiNi_xMn_yCo_{(1-x-y)}O_2$ experience 2–4% volume change across their functional range of operation,[126,127] while lithiated graphite, LiC_6, experiences up to 10%.[128,129] Si anodes can exhibit expansions of up to 400% depending on the state of lithiation.[130,131] In traditional liquid electrolyte systems, expansion/contraction effects primarily lead to failure through mechanical deformation of the SEI or electrochemical fracture of active particles.[132] Fracture of particles from large volume expansion is one example of failure that can occur in Si anodes.[130,133] For solid state systems, changes in volume can lead to physical delamination of the electrode-electrolyte interface and fracture of solid state components. Ultimately, this may limit accessible states of charge or cell power capability, which necessitates the development of internal/external methods to maintain contact during operation. However, the applicability of such methods may be limited since the ability to lithiate a host necessitates that the host has freedom to expand. Recently, Bucci et al. employed a finite element model to show how stress induced voltage shift in Si anode expansion in a stiff matrix can result in substantial capacity loss.[134] In subsequent work,[135] it was shown that the onset of micro-cracking in a SSE with elastic moduli

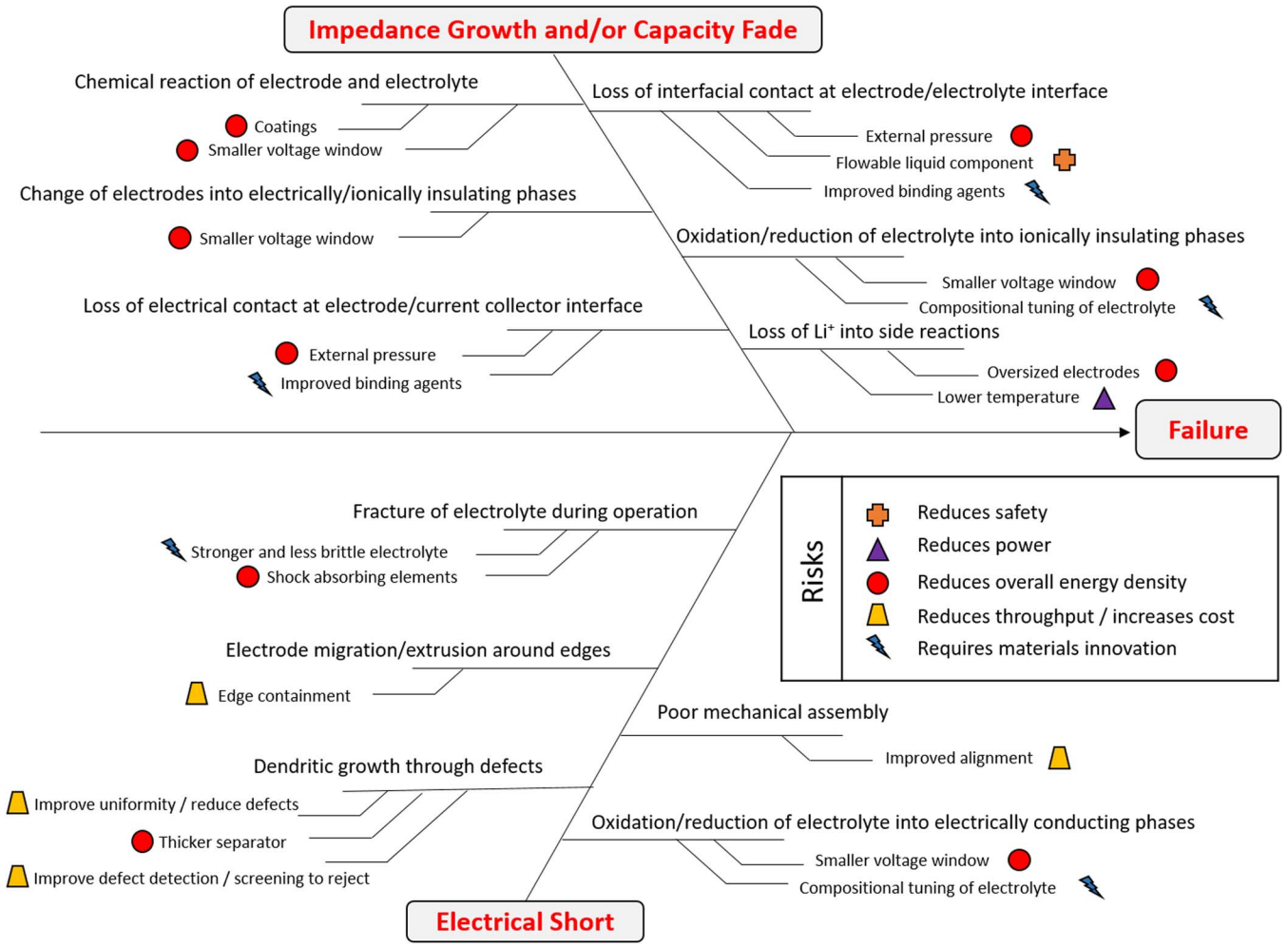

Figure 4. A basic fishbone diagram highlighting two of the key high level failure modes (impedance growth or electrical shorting) and the variety of potential contributing factors. Possible solutions and the consequent product risks to their implementation, including reduced safety, power, energy density, throughput, or requirement of material innovation are also shown. Understanding the interplay between material level issues and cell level ramifications are highlighted to reiterate holistic approaches.

and fracture toughness of LPS occurs at about 7.5% by volume expansion of the electroactive material, a limit that is near that of some electrodes.

Unlike polymer and liquid electrolyte systems where simply stacking and pressing electrode layers together is sufficient for developing and testing material systems, care must be taken to ensure quality Ohmic contact with SSEs. Cycling with heterogeneous contact points will result in local electric field non-uniformities. In the case of a metallic electrode, this may manifest itself via local current density distribution that could lead to a macroscopic avalanche development of low density microstructure.[136] This is detrimental for several reasons discussed below.

Non-uniform current density distribution.—The morphology of Li metal during cycling is dynamic,[137] unlike cycling through a host based anode such as silicon or carbon. The latter provide far fewer anode based cycling complexities at the expense of volumetric energy density at the product level. The formation of low density Li metal is undesirable as it reduces any volumetric advantage and introduces local current density non-uniformities at the anode-SSE interface.[136,138,139] Metallic heterogeneities are the root cause for developing electrical hot spots which may lead to electrical shorting failure mechanisms,[138,139] by potentially propagating pre-existing defects at the anode-SSE interface.[135] Coulombic efficiency is also negatively influenced by physical stranding of inaccessible metal caused by non-uniform plating and a low density microstructure, aptly described in the literature as 'dead Li'.[140,141] A distribution of current density will manifest as a distribution of C-rates, which may create a spectrum in depth of discharge within the cathode. In the absence of other dominant failure modes, this would result in capacity fade over long duty cycles. Motoyama et al. have experimentally shown heterogeneous Li metal plating on thin current collectors in contact with LiPON systems.[142–144] Spatially varying nucleation of Li metal at the electrolyte-current collector interface was observed to lead to bulging and even puncture of the current collector. Similarly, Yonemoto et al. recently reported impedance growth during Li symmetric-cell cycling, related to microstructural changes at the Li-LLZO interface,[145] reproduced in Figure 5. An approach to correct this microstructural damage was operating the cell at 100°C, thereby allowing the Li metal to retain a dense microstructure at the SSE interface.

Composite cathode matrices.—The compatibility of SSEs in contact with cathode active materials often stem from interactions of delithiated cathode materials at SSEs, particularly at elevated temperatures and voltages.[146] Intrinsically, many of the highest conductivity SSE systems are not thermodynamically stable in the voltage ranges of interest.[8,146,147] In sulfide systems, mutual diffusion of Co, P, and S at the interface have been predicted and observed using cross-sectional transmission electron microscopy.[148,149] For LLZO systems, $LiMnO_2$ forms readily at elevated temperature with manganese-containing

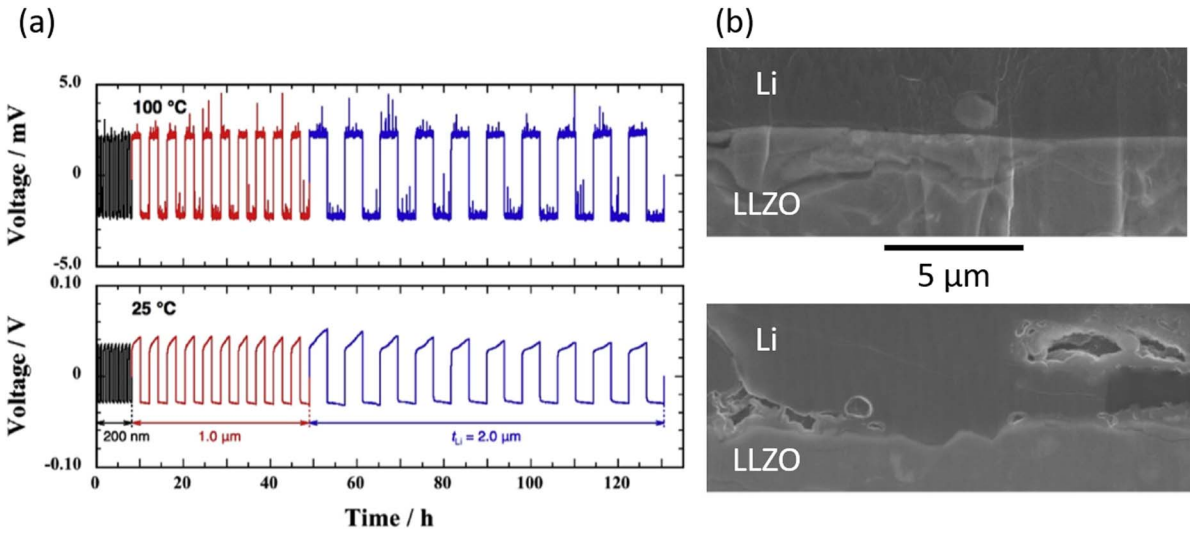

Figure 5. A representation of Li metal microstructural change based on Li|LLZO|Li symmetric cycling at 25 or 100°C. (a) Cycling profile at constant current, 0.1 mA cm^{-2}, of symmetric cells showing impedance gain, i.e. over-potential increase, during cycling at 25°C compared to the high temperature counterpart. (b) Corresponding scanning electron images of the Li-LLZO interface, highlighting microstructural change and low volume areas in Li metal for the sample cycled at low temperature. Images and plot were reproduced from Reference 145 with permission from Elsevier.

cathodes and further decomposes into additional interphases at the SSE-cathode interface.[146,150] Methods to control interdiffusion or reaction of SSEs and active material during high temperature processes or various duty cycle conditions are necessary to maintain theoretical capacity and minimize SSE-cathode interfacial impedance.

Some of the most practical studies to date enabling the integration of SSEs with cathodes have focused on the impact of protective active material coatings. Researchers from Samsung have shown that the addition of diamond-like carbon and Li_2ZrO_3 coatings are highly beneficial in improving the cycle life of $LiNi_xCo_yAl_{(1-x-y)}O_2$ cathodes with LPS electrolytes.[151–153] Other reports include $Li_4Ti_5O_{12}$ coated $LiNi_xCo_yAl_{(1-x-y)}O_2$ with LPS,[154] ZrO_2 coated $LiNi_xMn_yCo_{(1-x-y)}O_2$ with LPS,[155] $LiCO_3$ coated $LiCoO_2$ with LPS,[156] and Li_3PO_4 coated $LiNi_xMn_{2-x}O_4$ with LPS.[157] Many studies also utilize $LiNbO_3$ coated $LiCoO_2$ in contact with sulfide electrolytes.[4,158,159] SiO_2 has been demonstrated to form Li_2SiO_3 at the LPS-cathode boundary, which greatly reduces the interfacial resistance.[160] Protective coatings are bound by similar, albeit relaxed material property requirements to SSEs, including oxidative/reductive stability, high ionic conductivity, low electronic conductivity, chemical stability with materials in contact, and pragmatic processing.

The opportunity cost of a Li metal anode.—Gravimetric energy density or the theoretical volumetric energy density of Li metal are often key parameters discussed in the literature, but can be misleading when considering components that incur significant volume changes during the cell lifetime. From a realistic cell perspective, the dynamic morphology change of a Li metal or high Si content anodes can result in a buildup of cell pressure due to volume expansion.[136] Similarly, changes in the metal anode morphology due to cycling could reduce cell level energy density as well as introduce current density heterogeneity.[141,145] Due to these consequences, adequate attention must be paid to cell physical construction and components that may be needed in designs attempting to control anode morphology. Implementing engineered inactive components removes some of the volumetric or gravimetric advantages initially garnered by using a metal anode.

Fundamentally, the kinetic limitations of moving metal at solid interfaces has been previously investigated in some solid electrolyte systems.[161,162] Prior work on solid Li|LiI-Al_2O_3 interfaces by Jow and Liang shed light on physical limitations for metallic stripping occurring during discharge.[162] These findings indicate that there is a limit to the maximum current that can be drawn from a solid interface due to a self-diffusion limitation in the metal; i.e. the rate at which the metal is being depleted at the SSE interface is greater than the rate at which the bulk metal can fill vacancies. From a product perspective, this limits rate capability barring any other failure mode. Metallic alloys can be used to alleviate this issue by increasing the Li ion diffusion coefficient and mobility. Similar to other alloys,[163] this approach would incur a voltage and volume penalty associated compared to pure Li metal.

Failure by Li penetration through SSEs have been reported by a number of researchers;[9,34,35,164] some optical examples are reproduced in Figure 6. Though there have not been direct reports of penetration in every SSE family, it is likely that all systems are subject to similar Li metal related failure mechanisms. The post-mortem ex-situ detection of metal filaments may be difficult to characterize in some SSE compositions if they are unstable to reduction by Li causing the metal to be consumed in the electrolyte before they can be sufficiently characterized.[165] Though negatively affecting Coulombic efficiency, this mechanism of dendrite 'healing' could be viewed as an advantage. In liquid systems, this idea has been recently explored by using the parasitic reaction between Li polysulfides (Li_2S_x where $4 \leq x \leq 8$) and Li metal.[166] For future SSE systems, if Coulombic efficiency could be monitored accurately,[167] abnormal discrepancies might serve as a method to monitor the early stage of dendritic growth and prevent catastrophic failure at device level.[168]

Analogous to other electrically insulating materials, SSE systems are expected to have a fundamental material limit at which electrical failure will occur.[169–171] This could be through dielectric breakdown, electric field concentration due to rapid metal depletion at the interface,[162] mechanical flow of metal within existing defects developing increasing pressure,[172,173] or otherwise. Aguesse et al. have touched on key issues in a study on the origin of dendritic failure in Ga-doped LLZO;[34] highlighting the critical role of defects as a potential root cause for dendritic behavior and similarities to work in Na^+ systems exhibiting similar failure modes.[172,173] Porz et al.[31] experimentally show a correlation between surface defect population and Li metal penetration in four SSEs including amorphous 70/30 mol% Li_2S-P_2S_5, polycrystalline β-Li_3PS_4, and polycrystalline and single crystalline $Li_6La_3ZrTaO_{12}$. They analytically show that once a sharp crack has filled with electrodeposited lithium metal, the additional volume increase upon Li deposition is more easily accommodated by crack-opening than by extrusion of Li metal to the free surface. It was concluded that Li metal penetration behavior in SSEs is actually more

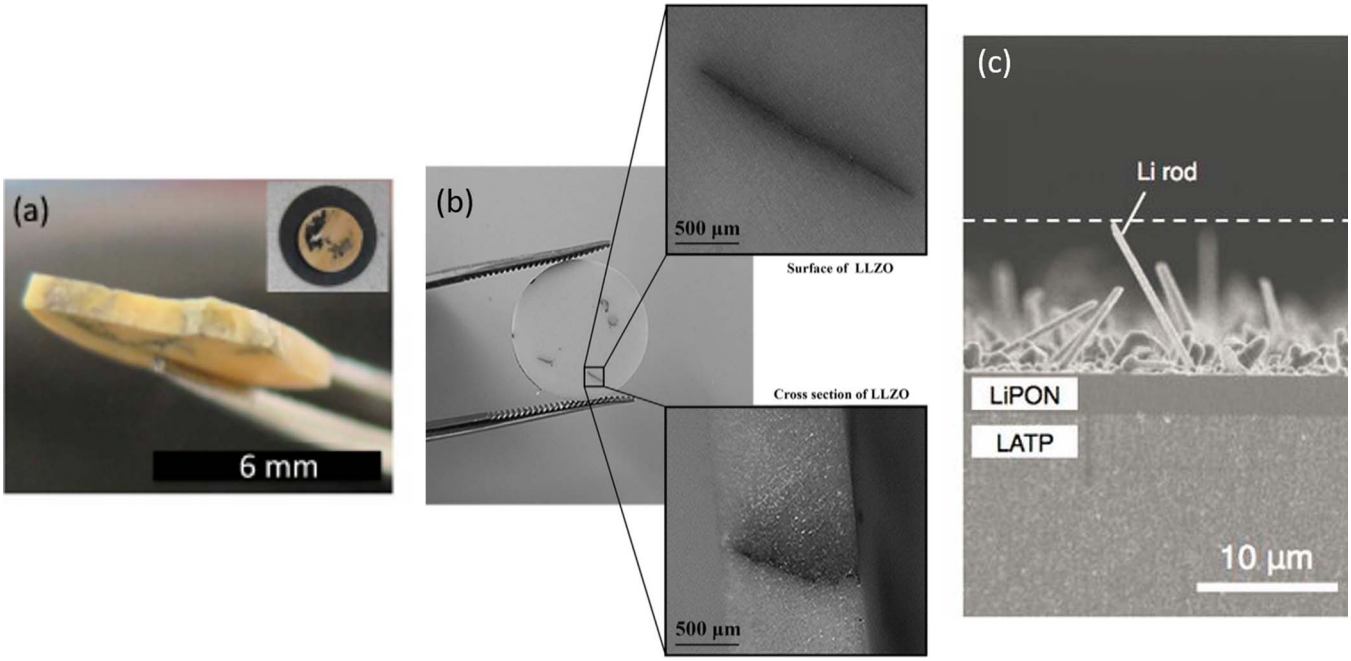

Figure 6. Reports of Li metal transverse dendrite failure mechanism in SSE materials. (a) Ga-doped LLZO studies cycling Li metal in Reference 34 used with permission from the American Chemical Society; (b) Al-doped LLZO samples after symmetric Li plating studies in Reference 9 reproduced with permission from Elsevier; and (c) cross sectional view of Li metal microstructure at a LiPON-Li interface from Reference 144 reproduced with permission from the Electrochemical Society.

Griffith-like than dendrite-like (i.e., originating from the amplification of interfacial fluctuations), as it depends critically on the surface flaw population. Theoretically expressing and experimentally determining the critical current density that is sustainable with high density, reproducible SSE material systems is of the utmost importance. Raj and Wolfenstein have developed a relationship between critical current density and dendritic nucleation.[174] Their preliminary work identifies conductivity as an important macroscopic material property to negate a Li penetration failure mode. Such a theory maintains consistency with a defect driven root cause failure mechanism, as increased conductivity would effectively reduce the magnitude of electric field at a particular crack tip, thus retarding propagation through the SSE.

While experimentally reporting negative results, such as failure statistics, is not prevalent in the literature, it is crucial to understand the limitations of SSEs and develop mechanistic frameworks that will shape future endeavors in this space. In LLZO, there has been some work showing that samples could only sustain up to 0.5 mA cm^{-2} before dendritic failure under room temperature symmetric Li cycling.[9,35,164,175] Engineering low defect density interfaces with very small Li|SSE resistance would greatly increase the ultimate current density sustainable.

Lateral dendritic growth is a higher order concern that should not be overlooked. In addition to adverse effects on Coulombic efficiency, without confinement lateral movement of metal could result in a shorting failure mode over the edge of the SSE. Product level mitigation strategies will likely involve the addition of extra materials or modification of existing components that could impact primary function, thereby lowering energy and/or power density in order to decrease the probability of a catastrophic failure. Such tradeoffs should be weighed accordingly when considering approaches to develop a robust product.

Development of Full Cells

Ultimately, advances in SSEs must be employed in full cell structures to exemplify their utility and substantiate the touted benefits. Integrating such structures requires understanding of material limitations, processing capabilities and importantly, cell form factor. Table I is presented as a summary of experimental efforts published in this context.

Cell architecture.—Integration of SSEs into full cell architectures can be done in several ways. Figure 7 outlines the main potential cell design architectures for all SSE families. The high conductivity of sulfide systems and macroscopic deformability make true solid state cells at high energy densities possible using cathodes with sulfide conducting material in the composite matrix.[21,79,89] Such cathodes can be integrated with the SSE in a number of ways including mechanical bonding. A number of research efforts have reported this type of architecture;[151–157,159,176–179] most notably, the development of $Li_{9.54}Si_{1.74}P_{1.33}S_{11.7}Cl_{0.3}$ for high temperature (100°C) and high rate (18C) cell demonstrations.[4] In all reports, the active cathode material electrode loading, typically ∼30–70 wt%, is strikingly less than traditional battery systems >90%.[180]

Interfacial contact.—Physically making adequate contact at both the anode-SSE interface as well as the cathode-SSE interface is nontrivial. The macroscopically deformable nature of sulfide systems provides a means of improving interfacial contact.[21,79,89] Pressure and temperature can be used to create low impedance interfaces with electrode materials. Conversely, the brittle nature of oxide systems negates the ability to use mechanical bonding to make Ohmic contact with low interfacial impedance without surface modification. Similar to LiPON based systems, thin film deposition of both anode and cathode components are possibilities though cost and scalability are of concern. Alternatively, surface modification of LLZO, such as ALD deposited ZnO or Ge, has been shown to be largely beneficial in enabling low interfacial resistance with high temperature bonded Li.[75,181,182] At room temperature, nearly negligible interfacial impedances and 1 Ω cm^2 have been shown for LPS|Li and LLZO|Li using best practices.[5,183]

Oxide systems have been shown in true solid state architecture by either growing a thin cathode atop LLZO,[184,185] or using a low melting point conducting agent such as Li_3BO_3 in the cathode.[186] A bulk co-sintering approach to create a bonded cathode-SSE interface introduces significant material compatibility issues during high temperature processing. It has been shown that a number of

Table I. A summary table of the efforts to develop a solid state battery cell in the literature.

SSE family	SSE material	SSE thick (μm)	Form	Cathode (Coating)	Active Mass Fraction (%)	Anode	Cell area (cm^2)	Test T (°C)	Achieved Capacity	Cycling Capability	Ref.
sulfide	$80Li_2S$-$20P_2S_5$	200	solid state	+NCA (Li_2ZrO_3)	60	graphite	46.6	25	110 mAh @ C/10, (120 mAh/g @ 0.05 mA/cm^2)	92% 100 cycles	152
sulfide	$75Li_2S$-$25P_2S_5$	-	solid state	+LCO ($LiNbO_3$)	70	graphite composite	-	60	1.55 mAh (105 mAh/g) @ C/10	65% 100 cycles	178
sulfide	$Li_{9.54}Si_{1.74}P_{1.44}S_{11.7}Cl_{0.3}$	240	solid state	+LCO ($LiNbO_3$)	60	LSPSCl - LTO	1	100	0.67 mAh (115 mAh/g) @ 18C	75% 500 cycles	4
sulfide	$80Li_2S$-$20P_2S_5$	-	solid state	+LMO (Li_3PO_4)	30	In	0.785	25	0.19 mAh (62 mAh/g) @ 0.064 mA/cm^2	10 cycles	157
sulfide	a-Li_3PS_4*	-	solid state	+NMC (ZrO_2)	59	$Li_{4.4}Si$	0.785	25	0.59 mAh (120 mAh/g) @ C/10	96% 50 cycles	155
sulfide	$70Li_2S$-$30P_2S_5$	-	solid state	+NCA ($Li_4Ti_5O_{12}$)	70	In	0.785	25	1.58 mAh (150 mAh/g @ 0.5 mA/cm^2)	-	154
sulfide	Li_3PO_4-Li_2S-SiS_2	1000	solid state	TiS_2	50	Li	0.785	25	0.5 mAh @ 0.063 mA/cm^2	50 cycles	87
oxide	Al_2O_3-$Li_7La_3Zr_2O_{12}$	1000	solid state	LCO	100	Li	1.33	25	-	-	184
oxide	Nb-$Li_7La_3Zr_2O_{12}$	1000	solid state	LCO	75	Li	1.13	25	0.167 (85 mAh/g) @ C/20	>99% 5 cycles	186
oxide	Nb-$Li_7La_3Zr_2O_{12}$	2000	solid state	LCO	100	Li	1.33	25	0.044 mAh (130 mAh/g) @C/10	98% 100 cycles	185
oxide	$Li_{6.25}Al_{0.25}La_3Zr_2O_{12}$	340	solid state	LTO	40	Li	1	95	0.064 (16 mAh/g) @ 0.008 mA/cm^2	>20 cycles	210
anti-perovskite	Li_3OCl	-	solid state	LCO	100	graphite	-	25	120 mAh/g @ 10 mA/g	55% 20 cycles	108
hydride	$LiBH_4$-LiI	1000	solid state	TiS_2	100	Li	1.23	120	226 mAh/g @ C/4	93% 50 cycles	211
hydride	$LiBH_4$-LiI	1200	solid state	LTO	80	Li	0.785	60	0.056 mAh (142 mAh/g @ 0.01 mA/cm^2)	80% 10 cycles	212
hydride	$LiBH_4$	1000	solid state	+LCO (Li_3PO_4)	100	Li	0.785	120	89 mAh/g @ 0.05 mA/cm^2	97% 30 cycles	213
nitride	Li_3N|PEO	1000	hybrid	TiS_2	50	Li	0.1	140	0.24 mAh @ C/1.2	50% 400 cycles	116
oxide	$Li_{6.75}La_3Zr_{1.75}Ta_{0.25}O_{12}$	1000	hybrid	LFP	75	Li	-	60	0.23 mAh (150 mAh/g) @ C/20	93% 100 cycles	194
oxide	Al-$Li_7La_3Zr_2O_{12}$	-	hybrid	LFP		Li	-	25	169 mAh/g @ 0.046C	5 cycles	36
oxide	LiF-$Li_{6.5}La_3Zr_{1.5}Ta_{0.5}O_{12}$	1200	hybrid	LFP	60	Li	0.385	65	0.27 mAh (142 mAh/g) @ 0.08 mA/cm^2	85% 100 cycles	192
oxide	$Li_7La_{2.75}Ca_{0.25}Zr_{1.75}Nb_{0.25}O_{12}$	200	hybrid	LFMO	80	Li	0.49	25	103 mAh/g @ C/10	>99% 50 cycles	5
oxide	$Li_7La_{2.75}Ca_{0.25}Zr_{1.75}Nb_{0.25}O_{12}$	300	hybrid	LFP	70	Li	0.785	20	0.084 mAh (132 mAh/g @ 0.1 mA/cm^2)	>91% 100 cycles	75
composite	$Li_7La_3Zr_2O_{12}$-PVdF	32	hybrid	LCO	85	graphite composite	10.6 (10 stacks)	25	670 mAh (148 mAh/g) @ C/2	91% 300 cycles	214
composite	$Li_{10}GeP_2S_{12}$-PEO	200-400	hybrid	LFP	-	Li	0.785	60	125 mAh/g @ 1C	90% 50 cycles	215
composite	$Li_7La_3Zr_2O_{12}$-SPEEK	3-5	hybrid	LFP	24	Li	-	25	160 mAh/g @ C/20	89% 100 cycles	216
composite	$Li_{6.75}La_3Zr_{1.75}Ta_{0.25}O_{12}$-PEO	70	hybrid	LFP	75	Li	0.746	60	5.8 mAh (156 mAh/g) @ 0.1 mA/cm^2	>99% 10 cycles	217
composite	$Li_{1.5}Al_{0.5}Ge_{1.5}(PO_4)_3$-PEO	-	hybrid	LFP	25	Li	0.69	100	3.5 mAh (140 mAh/g) @ 0.040 mA/cm^2 (C/87.5)	>90% 20 cycles	188

*Amorphous.
+Protective coating on active cathode particle utilized.
PEO: poly(ethylene oxide); PVdF: poly(vinylidene difluoride); SPEEK: sulfonated poly(ether ether ketone); NCA: $LiNi_xCo_yAl_{(1-x-y)}O_2$; LFP: $LiFePO_4$; LCO: $LiCoO_2$; NMC: $LiNi_xMn_yCo_{(1-x-y)}O_2$; LTO: $Li_4Ti_5O_{12}$; LMO: $LiNi_xMn_{2-x}O_4$; LFMO: $Li_2FeMn_3O_8$; Note that 100% active mass fraction indicates a thin film electrode.

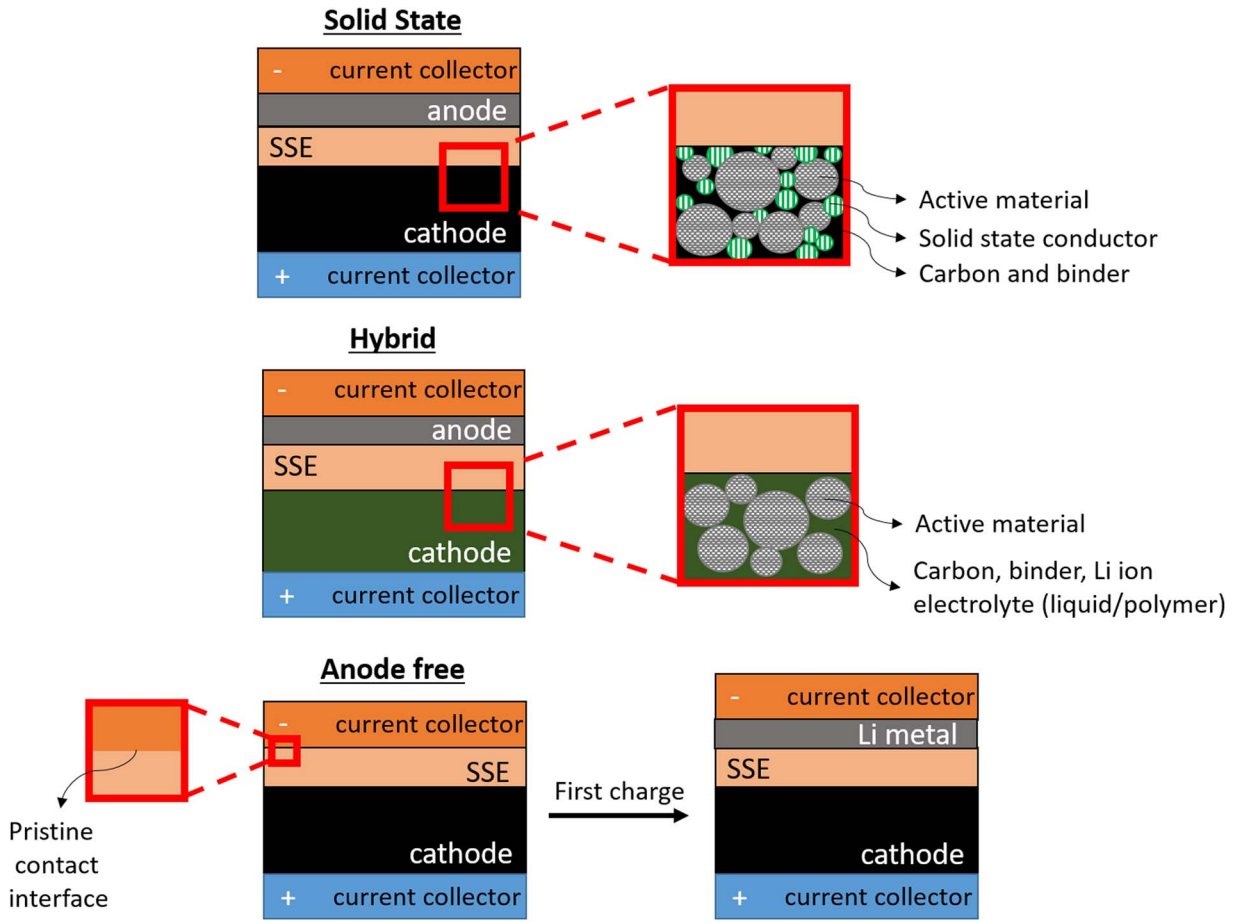

Figure 7. An illustration of main cell architectures utilized in solid state battery research to date. (a) All solid state configuration utilizing a solid state cathode interfaced with a solid electrolyte and high energy density solid anode; (b) a hybrid approach using a liquid or polymer based cathode interfaced with a solid electrolyte and high energy density anode; and (c) anode free design wherein the cell is constructed with only a cathode and separator while the metal anode is formed upon first charge. Cell performance, attributes, and pitfalls of both designs are discussed within the text and listed in Table I.

decomposition materials such as $La_2Zr_2O_7$, La_2O_3, La_3TaO_7, TiO_2, and $LaMnO_3$ form and are detrimental to interfacial impedance after fabrication.[146,150] Lower temperature densification and processing steps could be a valuable method to mitigate these effects.[187]

Broadly speaking, with the exception of thin film cathodes all reports of full cell architectures utilize lower active material electrode loading than state-of-the-art liquid cells. While the conductivity of SSE materials may be adequate for dense bodies utilized as electrolytes, it presents a limitation with respect to rate capability in composite solid state cathodes using such materials to draw Li ions in and out of the active material. Typical active material loadings in excess of 90 wt% are desired in cathode formulations.[180] The remainder is utilized for a combination of binding, electrical conduction, and ionic conduction. Polymeric binders, carbon, and liquid electrolytes having high conductivity and mobility are used in conventional cathodes. Liquid infiltration and wetting within the composite matrix enables rate capability to be limited by active material kinetics. In solid state systems, achieving a percolating network with high enough conductivity that persists in the presence of active material and high potential at relevant temperatures may ultimately limit full cell rate capabilities – a subtlety that is evident by numerous reports utilizing testing temperatures $>25^{\circ}C$ and active loadings of <85 wt%. Operation at lower rates may enable full capacity extraction in solid electrodes,[188] but practical applications require high rate capability. Enabling practical rate capabilities in thick, energy dense electrodes requires not only high conductivity materials, but also sufficiently large contact area amongst the particles or grains of ion conductors as well as between the ion conductors and the active materials in order to provide a percolating network for ion transport. In practice, this likely requires minimizing porosity within the electrode, which is a significant challenge when using a solid conductive matrix, though some porosity could be beneficial in allowing for volume expansion of the active material. A potential processing solution and benefit of residual connected porosity would be to infiltrate porous cathode structures with a slurry containing SSE material.[189] However, even higher conductivity than what has already been demonstrated in literature to date is desirable to enable high rate, high active loading solid state cathodes to account for reduced loading of solid ion conductor in the composite.

In some SSE systems, a hybrid architecture naturally emerges as a potential solution to rate capability and high temperature processing compatibility issues.[36,190,191] As schematically shown in Figure 7, some SSEs offer this prospective avenue for integration. While mechanical interfacing with cathode components is not an easily achievable feat for oxides due to their brittle nature, utilizing another ionic conductor in liquid or polymer phase, such as a gel,[191] makes a hybrid system possible. It is noted that although this is not a true solid state system and an ionically conductive salt is necessary, there may still be advantages to such a cell from a safety perspective by reducing the volume of flammable liquid electrolyte in comparison to a typical liquid system. Such an approach can also be utilized with a polymer or gel interfacing agent for the anode-SSE interface ensuring low interfacial resistance without the use of PVD methods or surface modification to make contact.[192,193] Unsurprisingly, this design approach introduces alternative cell level engineering challenges such as liquid confinement under cell pressure or liquid vapor pressure within a sealed apparatus. While these aspects will not be discussed in detail,

they warrant reflection when juxtaposing advantages of this type of architecture with traditional systems. Examples of the hybrid cathode integration approach have been shown with a poly(vinylidenene fluoride) cathode mixtures, leveraging the use of $Li(CF_3SO_2)_2N$ or $LiPF_6$ salt to gain a conductive matrix within the cathode and bonding layer between the cathode and LLZO.[192,194]

The most practically useful and energy dense cell design for a solid state system using a metal anode is an anode free architecture, similar in scheme to conventional graphite anode based cells. Unfortunately, this design has only been demonstrated in thin film form.[195] In this architecture, the cathode active material is fully discharged and lithiated. Upon the first charge, the anode is plated and subsequently cycled. Such a design requires intimate contact between the anode current collector and SSE prior to the first Li plating cycle and all subsequent cycles. As previously discussed, methods of making and maintaining contact may not be trivial. Leveraging methods from other fields to make electrical contact may provide insight to solving this challenge, such as metals deposited by PVD in the semiconductor industry or co-sintering of metals and ion conductors from the solid oxide fuel cell community.[71–74, 196] In addition to processing complexities introduced, factors such as propensity for alloy formation, plating morphology, contact continuity, and Li penetration into current collector metals require study. Reports have shown that Li nucleates in a highly non-uniform manner on various current collectors and can either puncture through a thin Cu metal layer or show finite solubility.[142,143,197] Coulombic efficiency without the use of excess Li must be maintained in excess of 99.99% for such a design to achieve acceptable cycle life.

Cycling behavior.—Cycle life ranging from 5–1000 has been demonstrated in various systems tested under numerous conditions. Table I summarizes the architecture, components, and cycling behavior of most reported results to date. LLZO full cells using the gel hybrid cell architecture approach have shown 100 cycles at C/20 with 93% capacity retention.[194] Small scale solid state LLZO full cells with $LiCoO_2$ (LCO) cathodes grown by PLD have demonstrated 98% capacity retention after 100 cycles at C/10.[185] Solid state LLZO cells employing the low melting point Li_3BO_3 oxide conductor within LCO cathode matrix show 85% capacity retention after 100 cycles at C/20.[186] While mechanisms for capacity degradation and low Coulombic efficiency have not been extensively studied, blocking interfacial SEI layers likely contribute to reduction of capacity and mechanisms for metal stranding account for a portion of Coulombic inefficiencies. Rate capability in oxide solid state cells need to be pushed into product relevant regimes >C/5 depending on application and Coulombic efficiencies must be significantly improved.

Sulfide full cell systems have been reported in a number of studies, with many cycling efforts at elevated temperature utilizing the Arrhenius dependence of conductivity for the solid state components. Using a $LiNbO_3$ protective cathode active particle coating and a modified sulfide SSE composition, researchers have been able to show steady cycling of solid state cells for 1000 cycles with about 75% capacity retention during testing at 100°C and fast discharge rates of 18C.[4] These results are encouraging and show promise for persistent development. This report utilized a 240 μm thick sulfide SSE. As discussed previously, substantial form factor reduction is necessary for competitive cell level energy densities.

Practically, care should be taken to be diligent about excess Li used in reports of Li metal cells. Akin to research in the early 1990s where excess Li metal was used to artificially maintain Coulombic efficiency as it was consumed,[198] little or no metal excess should be used as it will reduce cell energy density. Application specific testing would be useful to determine the path toward developing the most robust material systems. For example, slow, daily discharge cycles with an accompanying overnight charge cycle could be of value for mobile markets, whereas higher power applications relevant to automotive end use may separate candidate systems for potential future development.[199]

Cell energy density.—A claim of solid state batteries is the entitlement to ultimately achieve higher energy density compared to liquid counterparts. This originates from belief that solid state electrolytes can enable higher voltage cathodes or possibly energy dense lithium metal anodes. As previously discussed, the density of Li metal within full cells may be transient and can be reduced over many cycles.[141,145] A simple calculation of energy density from one of the few cells reporting all necessary parameters of those listed in Table I, assuming a nominal voltage of 3.8 V and no cell packaging, leads to a cell-level energy density of approximately 160 Wh L^{-1} for an all solid state sulfide architecture.[152] The work of Eroglu et al. highlights cell-level energy densities of approximately 250 and 700 Wh L^{-1} for consumer and transportation applications, respectively.[180] As Andre et al. point out, such high energy density at the cell level is necessary due to pack and system level penalties that will inevitably be incurred downstream.[200] Unfortunately, true cell energy densities are rarely reported in the literature and seldom are critical parameters such as electrode thicknesses discussed or presented in a manner that can be easily compared across varying studies.

Risks of Early Transition from R&D to Commercialization

Rapid progress in the development of SSEs and optimistic literature reviews give promise for devices that can push the frontier of Li ion batteries. However, the pursuit of higher energy density must be equally matched in focus on safety. All energy storage devices, including batteries, possess inherent risk as energy is being confined in a closed system that can be physically or electrically damaged. High profile examples of sparse abnormalities in battery components include the catastrophic fires that grounded Boeing's Dreamliner and decimated Samsung's Galaxy Note 7. These companies suffered substantial market capitalization losses after fielding battery related incidents reiterating the need for rigorous and thorough testing under realistic conditions before attempting to engage customers. Various automotive companies including Fisker,[201] Tesla,[202] and Balloré,[203] have had isolated examples of fire incidents. Similarly, consumer products such as laptops made by Dell[204] or HP[205] have been recalled due to hazards related to Li ion battery components. More recently, battery failures in hoverboards and e-cigarettes have also garnered substantial negative attention.[206,207] Efforts attempting to quickly transition Li metal anode using liquid and polymeric electrolyte have also been victim to unforeseen incidents. Moli energy batteries caused a fire in a mobile phone made by NTT due to Li metal dendriting, while Avestor's product employed a polymer electrolyte against Li metal that was responsible for explosions in AT&T's U-verse TV service.

Risk mitigation strategies such as smart battery management systems and software are powerful tools to contain electrochemical systems in a controlled manner. In emergency circumstances, engineering controls such as vents, shutdown separators, or diodes can offer an additional layer of protection.[47,208] In the case of Boeing, heavy steel cladding around the battery pack, which likely negated a substantial fraction of the energy benefit of Li-ion, was the accepted solution for its 787 Dreamliner.[209] Solid state systems offer a potential advantage in this regard. The safety characteristics in SSE systems (particularly reduced flammability compared to liquid systems) is a touted advantage and preliminary investigations using a custom micro cell for differential scanning calorimetry up to 400°C by Inoue and Mukai show that, in conditions where flammability is possible, the degree of safety in a solid state system may be advantageous compared to traditional systems since less total heat is generated.[6] However, it is important to continue to establish more rigorous analysis of solid state systems and to bring light to alternative failure modes that may not be present in conventional liquid electrolytes. Even the propensity of certain sulfide materials to produce toxic H_2S in the event of exposure to atmosphere could be a major roadblock toward commercialization. The energy density gains enabled by using potentially hazardous anode systems warrants deep contemplation. Akin to the complex development path of current battery technology,[198] solid state batteries will require development efforts of new, alternative and necessary

engineering controls to maintain safe operation in forthcoming applications. This section is meant to serve as a reminder that adequate research, testing, and validation must be executed before attempting to transition new technology into existing or novel product lines.

Enabling a sufficiently thin separator that maintains material properties with low defect density and relevant area, ∼10–100 cm^2, by utilizing a high throughput and low cost manufacturing scheme is a critical path gate that must be addressed for commercialization of a true solid state battery. Although SSEs may theoretically possess higher entitlement against metal dendriting than liquid counterparts, achieving reasonable manufacturing yield may be an enormous challenge. Sun et al. have outlined some of the preliminary solid state entrepreneurial and academic efforts in a recent review.[10] While there are a number of emerging technology companies attempting to make leaps from results akin to those in Table I to a viable product, pragmatic realization is potentially years to decades away.

Summary and Outlook

There has been incredible progress in the field of solid state electrolytes for Li ion batteries. The discussion in this work strongly emphasizes that, in the context of solid state battery technology, a holistic approach to material development, taking cell and product design considerations into account is powerful and necessary in creating resilient and far reaching solid state material technologies in the Li ion space. Highly conductive solid ionic materials have paved the way for the potentially ground breaking technology of high energy density anodes and a true solid state battery. Important interplay between processing, cell development, and materials physics have been discussed. Specific research vectors for advancing solid state battery technology include scalable manufacturing of low defect density thin ionic conducting solids, characterization methods to determine defect densities at relevant scales, increasing ionic conductivity of solid state electrolytes further, protective active cathode particle coatings, developing high ionic conductivity materials that are deformable or have low melting temperature, and increasing active cathode particle fraction in solid state electrodes.

Acknowledgments

VV and YMC gratefully acknowledge support from the U.S. Department of Energy, Energy Efficiency and Renewable Energy Vehicle Technologies Office under Award Number DE-EE0007810.

References

1. J. Janek and W. G. Zeier, *Nature Energy*, **1**, 16141 (2016).
2. S. LeVine, *The mysterious story of the battery startup that promised GM a 200-mile electric car*, in *Quartz*, (2013).
3. S. LeVine, *Sakti3's quest for a better battery: Hype, funding, promises, and then a surprise sale*, in *Quartz*, (2015).
4. Y. Kato, S. Hori, T. Saito, K. Suzuki, M. Hirayama, A. Mitsui, M. Yonemura, H. Iba, and R. Kanno, *Nature Energy*, **1**, 16030 (2016).
5. X. Han, Y. Gong, K. Fu, X. He, G. T. Hitz, J. Dai, A. Pearse, B. Liu, H. Wang, G. Rubloff, Y. Mo, V. Thangadurai, E. D. Wachsman, and L. Hu, *Nat Mater*, **16**, 572 (2017).
6. T. Inoue and K. Mukai, *ACS Appl. Mater. Interfaces*, **9**(2), 1507 (2017).
7. D. L. Wood Iii, J. Li, and C. Daniel, *Journal of Power Sources*, **275**, 234 (2015).
8. W. D. Richards, L. J. Miara, Y. Wang, J. C. Kim, and G. Ceder, *Chemistry of Materials*, **28**, 266 (2015).
9. A. Sharafi, H. M. Meyer, J. Nanda, J. Wolfenstine, and J. Sakamoto, *Journal of Power Sources*, **302**, 135 (2016).
10. C. Sun, J. Liu, Y. Gong, D. P. Wilkinson, and J. Zhang, *Nano Energy*, **33**, 363 (2017).
11. A. Manthiram, X. Yu, and S. Wang, *Nature Reviews Materials*, **2**, 16103 (2017).
12. K. Takada, *Acta Materialia*, **61**, 759 (2013).
13. R. Agrawal and G. Pandey, *Journal of Physics D: Applied Physics*, **41**, 223001 (2008).
14. E. Quartarone and P. Mustarelli, *Chemical Society Reviews*, **40**, 2525 (2011).
15. L. Baggetto, R. A. Niessen, F. Roozeboom, and P. H. Notten, *Advanced Functional Materials*, **18**, 1057 (2008).
16. J. G. Kim, B. Son, S. Mukherjee, N. Schuppert, A. Bates, O. Kwon, M. J. Choi, H. Y. Chung, and S. Park, *Journal of Power Sources*, **282**, 299 (2015).
17. J. F. M. Oudenhoven, L. Baggetto, and P. H. L. Notten, *Advanced Energy Materials*, **1**, 10 (2011).
18. J. C. Bachman, S. Muy, A. Grimaud, H.-H. Chang, N. Pour, S. F. Lux, O. Paschos, F. Maglia, S. Lupart, P. Lamp, L. Giordano, and Y. Shao-Horn, *Chemical Reviews*, **116**, 140 (2016).
19. A. B. Yaroslavtsev, *Russian Chemical Reviews*, **85**, 1255 (2016).
20. V. Thangadurai, S. Narayanan, and D. Pinzaru, *Chemical Society Reviews*, **43**, 4714 (2014).
21. D. Liu, W. Zhu, Z. Feng, A. Guerfi, A. Vijh, and K. Zaghib, *Materials Science and Engineering: B*, **213**, 169 (2016).
22. J. E. Ni, E. D. Case, J. S. Sakamoto, E. Rangasamy, and J. B. Wolfenstine, *Journal of Materials Science*, **47**, 7978 (2012).
23. J. Wolfenstine, H. Jo, Y.-H. Cho, I. N. David, P. Askeland, E. D. Case, H. Kim, H. Choe, and J. Sakamoto, *Materials Letters*, **96**, 117 (2013).
24. A. Sakuda, A. Hayashi, Y. Takigawa, K. Higashi, and M. Tatsumisago, *Journal of the Ceramic Society of Japan*, **121**, 946 (2013).
25. F. P. McGrogan, T. Swamy, S. R. Bishop, E. Eggleton, L. Porz, X. Chen, Y.-M. Chiang, and K. J. Van Vliet, *Advanced Energy Materials*, 1602011 (2017).
26. S. Smith, T. Thompson, J. Sakamoto, J. L. Allen, D. R. Baker, and J. Wolfenstine, *Solid State Ionics*, **300**, 38 (2017).
27. C. Monroe and J. Newman, *Journal of The Electrochemical Society*, **152**, A396 (2005).
28. A. Ferrese, P. Albertus, J. Christensen, and J. Newman, *Journal of The Electrochemical Society*, **159**, A1615 (2012).
29. Z. Ahmad and V. Viswanathan, arXiv 1702.08406, (2017).
30. R. D. Schmidt and J. Sakamoto, *Journal of Power Sources*, **324**, 126 (2016).
31. L. Porz, T. Swamy, H. Thaman, D. Rettenwander, T. Fromling, S. Berendts, R. Uecker, B. W. Sheldon, and Y.-M. Chiang, *Advanced Energy Materials*, Accepted (2017).
32. C. Xu, Z. Ahmad, A. Aryanfar, V. Viswanathan, and J. R. Greer, *Proceedings of the National Academy of Sciences*, **114**(1), 57 (2017) .
33. Y. Suzuki, K. Kami, K. Watanabe, A. Watanabe, N. Saito, T. Ohnishi, K. Takada, R. Sudo, and N. Imanishi, *Solid State Ionics*, **278**, 172 (2015).
34. F. Aguesse, W. Manalastas, L. Buannic, J. M. Lopez del Amo, G. Singh, A. Llordes, and J. A. Kilner, *ACS Appl. Mater. Interfaces*, **9**(4), 3808 (2017).
35. R. H. Basappa, T. Ito, and H. Yamada, *Journal of The Electrochemical Society*, **164**, A666 (2017).
36. S. Sugata, N. Saito, K. Watanabe, T. Ohnishi, J.-D. Kim, and I. Honma, *Meeting Abstracts*, **MA2016-02**, 849 (2016).
37. K. Minami, A. Hayashi, and M. Tatsumisago, *Journal of the American Ceramic Society*, **94**, 1779 (2011).
38. E. Yi, W. Wang, J. Kieffer, and R. M. Laine, *Journal of Materials Chemistry A*, **4**, 12947 (2016).
39. T. Thompson, S. Yu, L. Williams, R. D. Schmidt, R. Garcia-Mendez, J. Wolfenstine, J. L. Allen, E. Kioupakis, D. J. Siegel, and J. Sakamoto, *ACS Energy Letters*, 462 (2017).
40. W. Schafbauer, F. Schulze-Küppers, S. Baumann, W. A. Meulenberg, N. H. Menzler, H. P. Buchkremer, and D. Stöver, in *Materials Science Forum*, p. 1035 (2012).
41. K. Kerman and S. Ramanathan, *Journal of Materials Research*, **29**, 320 (2014).
42. Y. Zhao and L. L. Daemen, *Journal of the American Chemical Society*, **134**, 15042 (2012).
43. S.-i Orimo, Y. Nakamori, G. Kitahara, K. Miwa, N. Ohba, S.-i. Towata, and A. Züttel, *Journal of Alloys and Compounds*, **404**, 427 (2005).
44. B. D. McCloskey, *The journal of physical chemistry letters*, **6**, 4581 (2015).
45. P. Arora and Z. Zhang, *Chemical Reviews*, **104**, 4419 (2004).
46. J. W. Evans and L. C. De Jonghe, in *The Production and Processing of Inorganic Materials*, p. 402, Springer (2016).
47. C. P. Grey and J. M. Tarascon, *Nat Mater*, **16**, 45 (2017).
48. F. Langer, I. Bardenhagen, J. Glenneberg, and R. Kun, *Solid State Ionics*, **291**, 8 (2016).
49. J. Sakamoto, E. Rangasamy, H. Kim, Y. Kim, and J. Wolfenstine, *Nanotechnology*, **24**, 424005 (2013).
50. W. Xia, B. Xu, H. Duan, Y. Guo, H. Kang, H. Li, and H. Liu, *ACS Applied Materials & Interfaces*, **8**, 5335 (2016).
51. L. Cheng, E. J. Crumlin, W. Chen, R. Qiao, H. Hou, S. Franz Lux, V. Zorba, R. Russo, R. Kostecki, Z. Liu, K. Persson, W. Yang, J. Cabana, T. Richardson, G. Chen, and M. Doeff, *Physical Chemistry Chemical Physics*, **16**, 18294 (2014).
52. S. G. Kang and D. S. Sholl, *The Journal of Physical Chemistry C*, **118**, 17402 (2014).
53. P. M. Rice, W. D. Kingery, H. Bowen, D. R. Uhlmann, G. Y. Onoda, L. L. Hench, J. B. Wachtman, W. R. Cannon, and M. J. Matthewson, *Physical ceramics: principles for ceramic science and engineering*, (1997).
54. M. Rahaman and M. N. Rahaman, *Ceramic processing*, CRC press (2006).
55. E. Antoini, *Journal of Materials Science*, **27**, 3335 (1992).
56. Y. Kim, H. Jo, J. L. Allen, H. Choe, J. Wolfenstine, and J. Sakamoto, *J. Mater. Chem. A*, **4**, 12947 (2016).
57. A. I. Kingon and J. B. Clark, *Journal of the American Ceramic Society*, **66**, 253 (1983).
58. S. Lobe, C. Dellen, M. Finsterbusch, H.-G. Gehrke, D. Sebold, C.-L. Tsai, S. Uhlenbruck, and O. Guillon, *Journal of power sources*, **307**, 684 (2016).
59. S. Kim, M. Hirayama, S. Taminato, and R. Kanno, *Dalton Transactions*, **42**, 13112 (2013).
60. E. Hanc, W. Zając, L. Lu, B. Yan, M. Kotobuki, M. Ziąbka, and J. Molenda, *Chem. Mater.*, **29**(8), 3785 (2017).
61. A. C. Kozen, A. J. Pearse, C.-F. Lin, M. Noked, and G. W. Rubloff, *Chemistry of Materials*, **27**, 5324 (2015).

62. E. Kazyak, K.-H. Chen, K. N. Wood, A. L. Davis, T. Thompson, A. R. Bielinski, A. J. Sanchez, X. Wang, C. Wang, J. Sakamoto, and N. P. Dasgupta, *Chemistry of Materials*, **29**, 3785 (2017).
63. R.-J. Chen, M. Huang, W.-Z. Huang, Y. Shen, Y.-H. Lin, and C.-W. Nan, *Journal of Materials Chemistry A*, **2**, 13277 (2014).
64. X. Liu, J. Fu, and C. Zhang, *Nanoscale Research Letters*, **11**, 551 (2016).
65. C. Loho, R. Djenadic, M. Bruns, O. Clemens, and H. Hahn, *Journal of The Electrochemical Society*, **164**, A6131 (2017).
66. E. Yi, W. Wang, J. Kieffer, and R. M. Laine, *Journal of Power Sources*, **352**, 156 (2017).
67. K. E. Bastian, J. J. Burte, M. A. Cohn, C. N. Collins, J. P. DeGeorge, I. A. DiNunzio, R. C. Greenlese, A. Piciacchio, T. L. Pinto, and R. J. Sullivan, *Weighted sintering process and conformable load tile*, in, Google Patents (1999).
68. D. J. Dubetsky, *Method of achieving uniform sintering shrinkage in a laminated planar green ceramic substrate and apparatus therefor*, in, Google Patents (1981).
69. R. J. Gorte, S. Park, J. M. Vohs, and C. Wang, *Advanced Materials*, **12**, 1465 (2000).
70. S. Matsuda, Y. Kubo, K. Uosaki, and S. Nakanishi, *ACS Energy Letters*, **2**, 924 (2017).
71. K. Fu, Y. Gong, Y. Li, S. Xu, Y. Wen, L. Zhang, C. Wang, G. Pastel, J. Dai, B. Liu, H. Xie, Y. yao, E. Wachsman, and L. Hu, *Energy Environ. Sci.*, Accepted manuscript (2017).
72. P. L. Flaitz, A. M. Flanagan, J. M. Harvilchuck, L. W. Herron, J. U. Knickerbocker, R. W. Nufer, C. H. Perry, and S. N. Reddy, *Method and means for co-sintering ceramic/metal MLC substrates*, in, Google Patents (1993).
73. J. C. LaSalle and B. C. Sherman, *Co-sintering of similar materials*, in, Google Patents (2001).
74. G. B. Merrill, C. Schillig, A. J. Burns, and J. R. Paulus, *Material system of co-sintered metal and ceramic layers*, in, Google Patents (2015).
75. K. Fu, Y. Gong, B. Liu, Y. Zhu, S. Xu, Y. Yao, W. Luo, C. Wang, S. D. Lacey, J. Dai, Y. Chen, Y. Mo, E. Wachsman, and L. Hu, *Science Advances*, **3** (2017).
76. G. Sahu, Z. Lin, J. Li, Z. Liu, N. Dudney, and C. Liang, *Energy & Environmental Science*, **7**, 1053 (2014).
77. A. Hayashi, H. Muramatsu, T. Ohtomo, S. Hama, and M. Tatsumisago, *Journal of Materials Chemistry A*, **1**, 6320 (2013).
78. H. Muramatsu, A. Hayashi, T. Ohtomo, S. Hama, and M. Tatsumisago, *Solid State Ionics*, **182**, 116 (2011).
79. A. Hayashi, S. Hama, H. Morimoto, M. Tatsumisago, and T. Minami, *Journal of the American Ceramic Society*, **84**, 477 (2001).
80. H. Mio, J. Kano, and F. Saito, *Chemical Engineering Science*, **59**, 5909 (2004).
81. F. Mizuno, A. Hayashi, K. Tadanaga, and M. Tatsumisago, *Advanced Materials*, **17**, 918 (2005).
82. F. Mizuno, A. Hayashi, K. Tadanaga, and M. Tatsumisago, *Solid State Ionics*, **177**, 2721 (2006).
83. M. Tatsumisago and A. Hayashi, *International Journal of Applied Glass Science*, **5**, 226 (2014).
84. K. Takada, N. Aotani, and S. Kondo, *Journal of Power Sources*, **43**, 135 (1993).
85. S. Kondo, K. Takada, and Y. Yamamura, *Solid State Ionics*, **53–56, Part 2**, 1183 (1992).
86. N. Aotani, K. Iwamoto, K. Takada, and S. Kondo, *Solid State Ionics*, **68**, 35 (1994).
87. K. Iwamoto, N. Aotani, K. Takada, and S. Kondo, *Solid State Ionics*, **70**, 658 (1994).
88. Y. Seino, T. Ota, K. Takada, A. Hayashi, and M. Tatsumisago, *Energy & Environmental Science*, **7**, 627 (2014).
89. S. S. Berbano, M. Mirsaneh, M. T. Lanagan, and C. A. Randall, *International Journal of Applied Glass Science*, **4**, 414 (2013).
90. A. Sakuda, A. Hayashi, and M. Tatsumisago, *Scientific reports*, **3** (2013).
91. J. R. Akridge and H. Vourlis, *Solid State Ionics*, **18**, 1082 (1986).
92. E. Rangasamy, Z. Liu, M. Gobet, K. Pilar, G. Sahu, W. Zhou, H. Wu, S. Greenbaum, and C. Liang, *Journal of the American Chemical Society*, **137**, 1384 (2015).
93. H.-J. Deiseroth, S.-T. Kong, H. Eckert, J. Vannahme, C. Reiner, T. Zaiß, and M. Schlosser, *Angewandte Chemie International Edition*, **47**, 755 (2008).
94. S. Boulineau, M. Courty, J.-M. Tarascon, and V. Viallet, *Solid State Ionics*, **221**, 1 (2012).
95. J. H. Kennedy and Z. Zhang, *Solid State Ionics*, **28**, 726 (1988).
96. J. Kang and B. Han, *The Journal of Physical Chemistry Letters*, **7**, 2671 (2016).
97. M. R. Busche, D. A. Weber, Y. Schneider, C. Dietrich, S. Wenzel, T. Leichtweiss, D. Schröder, W. Zhang, H. Weigand, D. Walter, S. J. Sedlmaier, D. Houtarde, L. F. Nazar, and J. Janek, *Chemistry of Materials*, **28**, 6152 (2016).
98. S. D. Jones and J. R. Akridge, *Solid State Ionics*, **53**, 628 (1992).
99. A. Sakuda, A. Hayashi, S. Hama, and M. Tatsumisago, *Journal of the American Ceramic Society*, **93**, 765 (2010).
100. I. Repins, M. A. Contreras, B. Egaas, C. DeHart, J. Scharf, C. L. Perkins, B. To, and R. Noufi, *Progress in Photovoltaics: Research and Applications*, **16**, 235 (2008).
101. H. Kugai and N. Ota, *Method of forming thin film of inorganic solid electrolyte*, in, Google Patents (2003).
102. Y. Wang, Z. Liu, X. Zhu, Y. Tang, and F. Huang, *Journal of Power Sources*, **224**, 225 (2013).
103. K. H. Park, D. Y. Oh, Y. E. Choi, Y. J. Nam, L. Han, J. Y. Kim, H. Xin, F. Lin, S. M. Oh, and Y. S. Jung, *Adv. Mater.*, **28**, 1874 (2016).
104. S. Azuma, K. Aiyama, G. Kawamura, H. Muto, T. Mizushima, T. Uchikoshi, and A. Matsuda, *Journal of the Ceramic Society of Japan*, **125**, 287 (2017).
105. M. Braga, J. A. Ferreira, V. Stockhausen, J. Oliveira, and A. El-Azab, *Journal of Materials Chemistry A*, **2**, 5470 (2014).
106. M. Braga, N. Grundish, A. Murchison, and J. Goodenough, *Energy Environ. Sci.*, **10**, 331 (2017).
107. S. Stegmaier, J. Voss, K. Reuter, and A. C. Luntz, *Chem. Mater.*, **29**(10), 4330 (2017).
108. X. Lü, J. W. Howard, A. Chen, J. Zhu, S. Li, G. Wu, P. Dowden, H. Xu, Y. Zhao, and Q. Jia, *Adv. Sci.*, **3** (2016).
109. M. Menjo, H.-W. Li, M. Matsuo, K. Ikeda, and S.-i Orimo, *Journal of the Ceramic Society of Japan*, **117**, 457 (2009).
110. M. Matsuo and S.-i Orimo, *Advanced Energy Materials*, **1**, 161 (2011).
111. U. v Alpen, A. Rabenau, and G. H. Talat, *Applied Physics Letters*, **30**, 621 (1977).
112. B. A. Boukamp and R. A. Huggins, *Materials Research Bulletin*, **13**, 23 (1978).
113. H. Schulz and K. H. Thiemann, *Acta Crystallographica Section A*, **35**, 309 (1979).
114. H. Yamane, S. Kikkawa, and M. Koizumi, *Solid State Ionics*, **25**, 183 (1987).
115. T. Asai, K. Nishida, and S. Kawai, *Materials Research Bulletin*, **19**, 1377 (1984).
116. B. Knutz and S. Skaarup, *Solid State Ionics*, **18–19, Part 2**, 783 (1986).
117. R. Bittihn, *Solid State Ionics*, **8**, 83 (1983).
118. P. Hartwig, W. Weppner, and W. Wichelhaus, *Materials Research Bulletin*, **14**, 493 (1979).
119. P. O'hare and G. K. Johnson, *The Journal of Chemical Thermodynamics*, **7**, 13 (1975).
120. K. Iio, A. Hayashi, H. Morimoto, M. Tatsumisago, and T. Minami, *Chemistry of Materials*, **14**, 2444 (2002).
121. L. Zhan, Y. Zhang, X. Zhuang, H. Fang, Y. Zhu, X. Guo, J. Chen, Z. Wang, and L. Li, *Solid State Ionics*, **304**, 150 (2017).
122. Y. Zhu, X. He, and Y. Mo, *ACS Applied Materials & Interfaces*, **7**, 23685 (2015).
123. Y. Zhu, X. He, and Y. Mo, *Advanced Science*, 1600517 (2017).
124. A. C. Luntz, J. Voss, and K. Reuter, *The journal of physical chemistry letters*, **6**, 4599 (2015).
125. B. Xu, W. Li, H. Duan, H. Wang, Y. Guo, H. Li, and H. Liu, *Journal of Power Sources*, **354**, 68 (2017).
126. T. Ohzuku and A. Ueda, *Journal of The Electrochemical Society*, **141**, 2972 (1994).
127. N. Yabuuchi and T. Ohzuku, *Journal of Power Sources*, **119**, 171 (2003).
128. J. Dahn, *Physical Review B*, **44**, 9170 (1991).
129. Y. Reynier, R. Yazami, and B. Fultz, *Journal of power sources*, **165**, 616 (2007).
130. M. Obrovac and L. Christensen, *Electrochemical and Solid-State Letters*, **7**, A93 (2004).
131. M. Pharr, K. Zhao, X. Wang, Z. Suo, and J. J. Vlassak, *Nano letters*, **12**, 5039 (2012).
132. R. A. Huggins and W. D. Nix, *Ionics*, **6**, 57 (2000).
133. R. Dash and S. Pannala, *Scientific Reports*, **6**, 27449 (2016).
134. G. Bucci, T. Swamy, S. Bishop, B. W. Sheldon, Y.-M. Chiang, and W. C. Carter, *Journal of The Electrochemical Society*, **164**, A645 (2017).
135. G. Bucci, T. Swamy, Y.-M. Chiang, and W. C. Carter, ArXiv 1703.00113, (2017).
136. D. Wainwright and R. Shimizu, *Journal of Power Sources*, **34**, 31 (1991).
137. N. J. Dudney, *J Electroceram*, 1 (2017).
138. J. Lang, L. Qi, Y. Luo, and H. Wu, *Energy Storage Materials*, **7**, 115 (2017).
139. W. Xu, J. Wang, F. Ding, X. Chen, E. Nasybulin, Y. Zhang, and J.-G. Zhang, *Energy & Environmental Science*, **7**, 513 (2014).
140. D. Santhanagopalan, D. Qian, T. McGilvray, Z. Wang, F. Wang, F. Camino, J. Graetz, N. Dudney, and Y. S. Meng, *The Journal of Physical Chemistry Letters*, **5**, 298 (2014).
141. K.-H. Chen, K. N. Wood, E. Kazyak, W. S. LePage, A. L. Davis, A. J. Sanchez, and N. P. Dasgupta, *J. Mater. Chem. A*, Advance article (2017).
142. M. Motoyama, M. Ejiri, and Y. Iriyama, *Electrochemistry*, **82**, 364 (2014).
143. M. Motoyama, M. Ejiri, and Y. Iriyama, *Journal of The Electrochemical Society*, **162**, A7067 (2015).
144. R. Tsukamoto, F. Yonemoto, M. Motoyama, and Y. Iriyama, *Meeting Abstracts*, **MA2016-02**, 4116 (2016).
145. F. Yonemoto, A. Nishimura, M. Motoyama, N. Tsuchimine, S. Kobayashi, and Y. Iriyama, *Journal of Power Sources*, **343**, 207 (2017).
146. L. Miara, A. Windmüller, C.-L. Tsai, W. D. Richards, Q. Ma, S. Uhlenbruck, O. Guillon, and G. Ceder, *ACS Applied Materials & Interfaces*, **8**, 26842 (2016).
147. Y. Zhu, X. He, and Y. Mo, *Journal of Materials Chemistry A*, **4**, 3253 (2016).
148. A. Sakuda, A. Hayashi, and M. Tatsumisago, *Chemistry of Materials*, **22**, 949 (2010).
149. J. Haruyama, K. Sodeyama, and Y. Tateyama, *ACS Appl. Mater. Interfaces*, **9**(1), 286 (2017).
150. J. Wakasugi, H. Munakata, and K. Kanamura, *Electrochemistry*, **85**, 77 (2017).
151. Y. Aihara, S. Ito, R. Omoda, T. Yamada, S. Fujiki, T. Watanabe, Y. Park, and S. Doo, *Frontiers in Energy Research*, **4**, 18 (2016).
152. S. Ito, S. Fujiki, T. Yamada, Y. Aihara, Y. Park, T. Y. Kim, S.-W. Baek, J.-M. Lee, S. Doo, and N. Machida, *Journal of Power Sources*, **248**, 943 (2014).
153. H. Visbal, Y. Aihara, S. Ito, T. Watanabe, Y. Park, and S. Doo, *Journal of Power Sources*, **314**, 85 (2016).
154. Y. Seino, T. Ota, and K. Takada, *Journal of Power Sources*, **196**, 6488 (2011).
155. N. Machida, J. Kashiwagi, M. Naito, and T. Shigematsu, *Solid State Ionics*, **225**, 354 (2012).
156. J. Kim, M. Kim, S. Noh, G. Lee, and D. Shin, *Ceramics International*, **42**, 2140 (2016).
157. S. Yubuchi, Y. Ito, T. Matsuyama, A. Hayashi, and M. Tatsumisago, *Solid State Ionics*, **285**, 79 (2016).
158. N. Kamaya, K. Homma, Y. Yamakawa, M. Hirayama, R. Kanno, M. Yonemura, T. Kamiyama, Y. Kato, S. Hama, and K. Kawamoto, *Nature materials*, **10**, 682 (2011).
159. N. Ohta, K. Takada, I. Sakaguchi, L. Zhang, R. Ma, K. Fukuda, M. Osada, and T. Sasaki, *Electrochemistry communications*, **9**, 1486 (2007).
160. A. Sakuda, H. Kitaura, A. Hayashi, K. Tadanaga, and M. Tatsumisago, *Journal of The Electrochemical Society*, **156**, A27 (2009).
161. R. Armstrong and B. Horrocks, *Solid State Ionics*, **94**, 181 (1997).
162. T. R. Jow and C. C. Liang, *Journal of The Electrochemical Society*, **130**, 737 (1983).
163. R. A. Huggins, *Journal of Power Sources*, **81–82**, 13 (1999).

164. R. Sudo, Y. Nakata, K. Ishiguro, M. Matsui, A. Hirano, Y. Takeda, O. Yamamoto, and N. Imanishi, *Solid State Ionics*, **262**, 151 (2014).
165. P. Bron, B. Roling, and S. Dehnen, *Journal of Power Sources*, **352**, 127 (2017).
166. W. Li, H. Yao, K. Yan, G. Zheng, Z. Liang, Y.-M. Chiang, and Y. Cui, *Nature Communications*, **6**, Article number 7436 (2015).
167. P. Ladpli, F. Kopsaftopoulos, R. Nardari, and F.-K. Chang, in, p. 1017108 (2017).
168. S. V. Sazhin, E. J. Dufek, and K. L. Gering, *Journal of The Electrochemical Society*, **164**, A6281 (2017).
169. C. Zener, *Proceedings of the Royal Society of London. Series A, Containing Papers of a Mathematical and Physical Character*, **145**, 523 (1934).
170. K. Kerman and S. Ramanathan, *Journal of Applied Physics*, **115**, 174307 (2014).
171. I.-C. Chen, S. E. Holland, and C. Hu, *IEEE Journal of Solid-State Circuits*, **20**, 333 (1985).
172. R. D. Armstrong, T. Dickinson, and J. Turner, *Electrochimica Acta*, **19**, 187 (1974).
173. L. C. De Jonghe, L. Feldman, and A. Beuchele, *Journal of Materials Science*, **16**, 780 (1981).
174. R. Raj and J. Wolfenstine, *Journal of Power Sources*, **343**, 119 (2017).
175. K. Ishiguro, Y. Nakata, M. Matsui, I. Uechi, Y. Takeda, O. Yamamoto, and N. Imanishi, *Journal of The Electrochemical Society*, **160**, A1690 (2013).
176. H. Kitaura, A. Hayashi, T. Ohtomo, S. Hama, and M. Tatsumisago, *Journal of Materials Chemistry*, **21**, 118 (2011).
177. T. Inada, T. Kobayashi, N. Sonoyama, A. Yamada, S. Kondo, M. Nagao, and R. Kanno, *Journal of Power Sources*, **194**, 1085 (2009).
178. T. Ohtomo, A. Hayashi, M. Tatsumisago, Y. Tsuchida, S. Hama, and K. Kawamoto, *Journal of Power Sources*, **233**, 231 (2013).
179. B. R. Shin, Y. J. Nam, D. Y. Oh, D. H. Kim, J. W. Kim, and Y. S. Jung, *Electrochimica Acta*, **146**, 395 (2014).
180. D. Eroglu, K. R. Zavadil, and K. G. Gallagher, *Journal of The Electrochemical Society*, **162**, A982 (2015).
181. C. Wang, Y. Gong, B. Liu, K. Fu, Y. Yao, E. Hitz, Y. Li, J. Dai, S. Xu, W. Luo, E. D. Wachsman, and L. Hu, *Nano Lett.*, **17**(1), 565 (2017).
182. W. Luo, Y. Gong, Y. Zhu, Y. Li, Y. Yao, Y. Zhang, K. Fu, G. Pastel, C.-F. Lin, Y. Mo, E. D. Wachsman, and L. Hu, *Advanced Materials*, 1606042 (2017).
183. L. Cheng, W. Chen, M. Kunz, K. Persson, N. Tamura, G. Chen, and M. Doeff, *ACS applied materials & interfaces*, **7**, 2073 (2015).
184. M. Kotobuki, K. Kanamura, Y. Sato, and T. Yoshida, *Journal of Power Sources*, **196**, 7750 (2011).
185. S. Ohta, T. Kobayashi, J. Seki, and T. Asaoka, *Journal of Power Sources*, **202**, 332 (2012).
186. S. Ohta, S. Komagata, J. Seki, T. Saeki, S. Morishita, and T. Asaoka, *Journal of Power Sources*, **238**, 53 (2013).
187. S. S. Berbano, J. Guo, H. Guo, M. T. Lanagan, and C. A. Randall, *J. Am. Ceram Soc.*, **100**, 2123 (2017).
188. A. Kubanska, L. Castro, L. Tortet, M. Dollé, and R. Bouchet, *J. Electroceram.*, 1 (2017).
189. D. H. Kim, D. Y. Oh, K. H. Park, Y. E. Choi, Y. J. Nam, H. A. Lee, S.-M. Lee, and Y. S. Jung, *Nano Lett.*, **17**(5), 3013 (2017).
190. L. Liu, X. Qi, Q. Ma, X. Rong, Y.-S. Hu, Z. Zhou, H. Li, X. Huang, and L. Chen, *ACS Applied Materials & Interfaces*, **8**, 32631 (2016).
191. B. Liu, Y. Gong, K. Fu, X. Han, Y. Yao, G. Pastel, C. Yang, H. Xie, E. D. Wachsman, and L. Hu, *ACS Appl. Mater. Interfaces*, **9**(22), 18809 (2017).
192. Y. Li, B. Xu, H. Xu, H. Duan, X. Lü, S. Xin, W. Zhou, L. Xue, G. Fu, A. Manthiram, and J. B. Goodenough, *Angewandte Chemie*, **129**, 771 (2016).
193. P. R. Chinnam and S. L. Wunder, *ACS Energy Lett.*, **2**(1) 134 (2017).
194. F. Du, N. Zhao, Y. Li, C. Chen, Z. Liu, and X. Guo, *Journal of Power Sources*, **300**, 24 (2015).
195. B. J. Neudecker, N. J. Dudney, and J. B. Bates, *Journal of The Electrochemical Society*, **147**, 517 (2000).
196. W. Z. Zhu and S. C. Deevi, *Materials Science and Engineering: A*, **362**, 228 (2003).
197. S. C. Nagpure, R. G. Downing, B. Bhushan, and S. Babu, *Scripta Materialia*, **67**, 669 (2012).
198. G. E. Blomgren, *Journal of The Electrochemical Society*, **164**, A5019 (2017).
199. A. F. Burke, *Proceedings of the IEEE*, **95**, 806 (2007).
200. D. Andre, S.-J. Kim, P. Lamp, S. F. Lux, F. Maglia, O. Paschos, and B. Stiaszny, *Journal of Materials Chemistry A*, **3**, 6709 (2015).
201. C. Jensen, *Fisker recalling 239 karma plug-in hybrids for fire hazard*, in New York Times (2011).
202. C. Jensen, *Tesla says car fire started in battery*, in New York Times (2013).
203. L. Masson, *Two autolib electric cars burn down in Paris*, in Plug-in Cars (2013).
204. CSPC, *Dell announces recall of notebook computer batteries due to fire hazard*, in United States Consumer Product Safety Commission (2006).
205. CSPC, *HP recalls batteries for HP and Compaq notebook computers due to fire and burn hazards*, in United States Consumer Product Safety Commission (2016).
206. R. Abrams, *Fire Risk Prompts Safety Agency to Recall Some Hoverboards*, in New York Times (2016).
207. H. Weisbaum, *What's Causing Some E-Cigarette Batteries to Explode?*, *in NBC News*, (2016).
208. D. Doughty and E. P. Roth, *Electrochemical Society Interface*, **21**, 37 (2012).
209. J. Mouawad, *Report on Boeing 787 dreamliner battery flaws finds lapses at multiple points*, in New York Times (2014).
210. J. van den Broek, S. Afyon, and J. L. M. Rupp, *Advanced Energy Materials*, **6**, 1600736 (2016).
211. H. Wang, C. Ma, M. Chi, and C. Liang, *Adv. Mater. Interfaces*, **2**, 1500268 (2015).
212. D. Sveinbjörnsson, A. S. Christiansen, R. Viskinde, P. Norby, and T. Vegge, *Journal of The Electrochemical Society*, **161**, A1432 (2014).
213. K. Takahashi, K. Hattori, T. Yamazaki, K. Takada, M. Matsuo, S. Orimo, H. Maekawa, and H. Takamura, *Journal of Power Sources*, **226**, 61 (2013).
214. Y.-C. Jung, S.-K. Kim, M.-S. Kim, J.-H. Lee, M.-S. Han, D.-H. Kim, W.-C. Shin, M. Ue, and D.-W. Kim, *Journal of Power Sources*, **293**, 675 (2015).
215. S. Chen, Y. Zhao, J. Yang, L. Yao, and X. Xu, *Ionics*, 1 (2016).
216. X. Yan, Z. Li, Z. Wen, and W.-Q. Han, *The Journal of Physical Chemistry C*, **121**, 1431 (2017).
217. R.-J. Chen, Y.-B. Zhang, T. Liu, B.-Q. Xu, Y.-H. Lin, C.-W. Nan, and Y. Shen, *ACS Applied Materials & Interfaces*, **9**, 9654 (2017).